universität wien

MASTERARBEIT

Titel der Masterarbeit

„Modulation of the MAPK pathway by differential nano-spatial distribution of ephrins to Eph receptors“

verfasst von

Dominik Lindenhofer BSc

angestrebter akademischer Grad

Master of Science (MSc)

Wien, 2015

Studienkennzahl lt. Studienblatt:	A 066 830
Studienrichtung lt. Studienblatt:	Masterstudium Molekulare Biologie
Betreut von:	Ao. Univ.-Prof. Dr. Friedrich Propst

Abstract

The Eph receptor family, the largest family of receptor tyrosine kinases, is involved in cell-cell communication and is activated by cell surface-associated ephrin ligands. Nano-spatial distribution of ephrin-A5 ligands was shown to cause differential phosphorylation of the EphA2 receptor and to regulate the invasive properties of MDA-MB-231 cells, a human breast cancer cell line. Here we investigated the initial responses of MDA-MB-231 cells upon treatment with clustered ephrin-A5 on the known target pathway HRas-Erk. We established a system that will enable us to identify the causative intracellular effects leading to this differential response of invasiveness elicited by varying nano-spatially distributed ephrin-A5 ligands.

Die Eph Rezeptor Familie, die größte der Rezeptor-Tyrosinkinasen, spielt eine Rolle in Zell-Zell Kommunikation und wird durch Ephrine, welche an die Zelloberfläche gebunden sind, aktiviert. Es wurde gezeigt, dass die Anordnung von Ephrin-A5 Liganden in nano-räumlicher Art und Weise die Phosphorylierung von EphA2 Rezeptoren und die invasiven Fähigkeiten von MDA-MB-231 Zellen modulieren. Wir haben die unmittelbaren Reaktionen von MDA-MB-231 Zellen auf geclusterte Ephrin-A5 Liganden im Bezug auf den HRas-Erk Signalweg untersucht. Wir haben ein System geschaffen, welches uns erlaubt die intrazellulären Effekte zu untersuchen, welche zu der unterschiedlichen invasiven Reaktion nach Stimulation mit unterschiedlich nano-räumlich variierten Ephrin-A5 Liganden führt.

Content

Abstract 1

1. **Introduction** 4

1.1. Eph receptor/ephrin signalling *4*

1.1.1. Structure of the Eph receptors 4

1.1.2. Activation of Eph receptors 5

1.1.3. Ligand-independent functions of Eph receptors 7

1.1.4. Cellular effects after activation of Eph receptors 9

1.1.5. Ephrin-A1 induced signalling mediated by EphA2 in the context of cancer 13

1.2. DNA origami – Nanocalipers *15*

1.3. Proximity ligation assay *17*

2. **Project outline** 18

3. **Materials and Methods** 21

3.1. Cell Culture *21*

3.2. Stimulation of Eph receptors *21*

3.3. Proximity Ligation Assay *22*

3.4. Immunocytochemistry (ICC) *25*

3.5. RNA isolation and RT-qPCR *26*

3.6. Statistical analysis *27*

4. **Results** 28

4.1. Stimulation with IgG-clustered ephrin-A5 causes tyrosine-phosphorylation of the EphA2 receptor *28*

4.2. Elevated levels of Erk and pErk after stimulation with IgG-clustered ephrin-A5 *31*

4.3. Treatment with clustered ephrin-A5 causes c-FOS activation *35*

4.4. RT-qPCR results on RNA from individual experiments show similar trend compared to RT-qPCR results from equally pooled RNA of these individual experiments *40*

4.5. Ephrin-A5 nanocalipers mediate tyrosine-phosphorylation of the EphA2 receptor 41

5. **Discussion** 44

5.1. Improvement in the extent of EphA2 receptor tyrosine-phosphorylation 44

5.2. Clustering of Erk is induced after treatment with IgG-clustered ephrin-A5 44

5.3. Expression profiles of genes investigated serve as references for RNA-seq experiments 45

5.4. Reduction in RNA-seq experiments through pooling of RNA 46

5.5. NC40 shows higher potential to cause EphA2 tyrosine-phosphorylation than NC0 and NC100 46

5.6. Future perspectives 47

6. **Acknowledgments** 48

7. **References** 49

1. Introduction

1.1. Eph receptor/ephrin signalling

Receptor-mediated signalling is a complex process, which allows cells to communicate in their direct microenvironment. These receptors are activated by ligands presented in the microenvironment and induce signal cascades eliciting various cellular responses including growth, migration, survival and differentiation.

The erythropoietin-producing hepatocellular carcinoma (Eph) receptor family, the largest family of receptor tyrosine kinases, is involved in cell-cell communication and is activated by cell surface-associated Eph receptor-interacting protein (ephrin) ligands. The human genome contains nine EphA receptors, which bind preferably to five glycosylphosphatidylinositol (GPI)-linked ephrin-A ligands; and five EphB receptors predominantly binding three transmembrane ephrin-B ligands. While there is strict intra-subclass specificity, there are some exceptions such as the interaction between EphA4 to ephrin-Bs and EphB2 to ephrin-A5. Moreover, EphB4 almost exclusively binds to ephrin-B2 (Pasquale, 2010).

1.1.1. Structure of the Eph receptors

On a structural level, Eph receptors contain an amino-terminal ephrin binding domain, a cysteine-rich region with a Sushi domain, two fibronectin III repeats followed by the cytoplasmic domain consisting of a Src homology 2 (SH2) binding site, a juxtamembrane region, a tyrosine kinase domain, a sterile alpha motif (SAM) domain and a PSD95, DLG, ZO1 (PDZ) binding motif (Fig. 1). The juxtamembrane region regulates the kinase activity of the Eph receptor and can bind to interacting proteins (Pasquale, 2008). The SAM domain and the PDZ binding motif also interact with various proteins that are crucial for signalling and the function of the Eph receptor (Pasquale, 2010). In addition, the kinase domain is able to interact with certain guanine nucleotide exchange factors (GEFs) for Rho family GTPases (Noren and Pasquale, 2004).

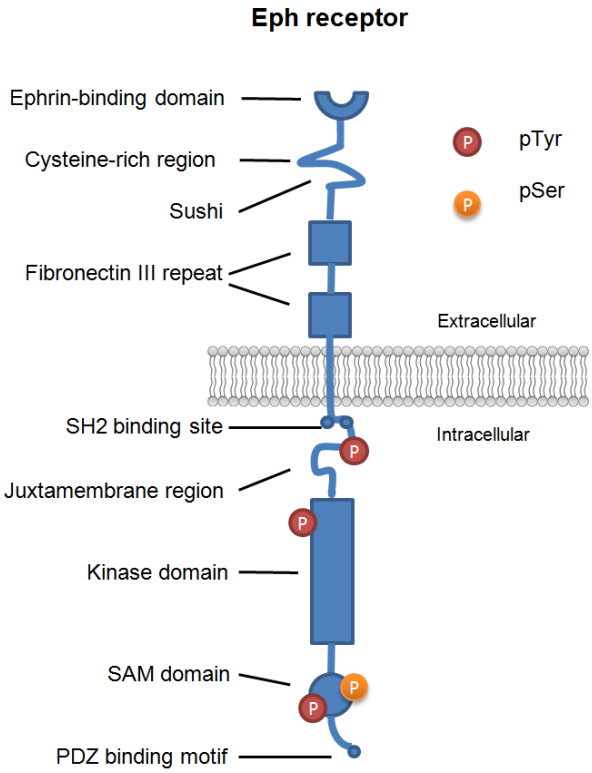

Figure 1: Structure of Eph receptor consisting extracellularly of an ephrin-binding domain, a cysteine-rich region with Sushi and two fibronectin III repeats. Intracellularly the receptor possesses SH2 binding sites, a juxtamembrane region, a kinase domain, a SAM domain and a PDZ binding motif.

1.1.2. Activation of Eph receptors

Interaction of the Eph receptor with its ligands initiates the clustering and formation of a signalling complex. Signal transduction can occur both in the direction of the receptor (forward signalling) and that of the ligand (reverse signalling). Forward signalling involves the kinase activity of the respective Eph receptor, whereas reverse signalling is dependent on the Src kinase family (Boyd et al., 2014). It was reported that when recombinant ephrins are used to treat Eph receptor expressing cells, only ephrins that are artificially-clustered or membrane-bound can effectively elicit forward signalling (Davis et al., 1994). In contrast to these findings, a functional role for soluble monomeric and unclustered ephrin-A1 was suggested (Beauchamp and Debinski, 2012). It was shown that it is cleaved from the surface of cancer cells that are expressing ephrin-A1 and is capable of inducing phosphorylation and internalisation of EphA2 receptors in glioblastoma multiforme (GBM) cells, albeit at

lower levels than clustered ephrin-A1. It was further proposed that soluble monomeric ephrin-A1 might have a function in paracrine signalling (Wykosky et al., 2008). Another study found soluble ephrin-A1 to be released from breast adenocarcinoma and HeLa cells and highlighted its requirement for the growth of those cancer cells (Alford et al., 2010). Moreover, soluble monomeric ephrin-A1 was identified in the serum of patients with hepatocellular carcinoma and was suggested as a potential biomarker for malignancy (Cui et al., 2010).

After binding of the ephrin ligand to the respective Eph receptor, tetrameric signalling units consisting of four Eph receptors and four ephrin ligands can initiate further clustering and cause cross-phosphorylation of tyrosine residues on the Eph receptors. Eph receptors that are both bound and not bound to ligands can further interact with the initial tetrameric signalling unit via the cysteine-rich region and this can lead to the formation of multimeric signalling clusters (Boyd et. al, 2014)

The Tyrosine residues that are predominately phosphorylated in the EphA2 receptor are Tyr^{587} and Tyr^{593} in the juxtamembrane domain; Tyr^{734} and Tyr^{771} in the kinase domain; and Tyr^{929} in the SAM domain. $pTyr^{587}$ and $pTyr^{593}$ interact with the Vav2/3 GEFs, whereas the p85 subunit of PI3K binds to $pTyr^{734}$. Both Vav3 GEF and p85 can bind to $pTyr^{929}$. Although Tyr^{929} was not found to be phosphorylated in an *in vitro* kinase assay, studies show that mutations at this residue impair ephrin-A1 induced vascular assembly of endothelial cells. However, it was suggested that it might be phosphorylated in other cell types or by kinases other than EphA2 (Fang et al., 2008). Furthermore, Grb10 and low molecular weight protein-tyrosine phosphatase (LMW-PTP) bind to EphB1 at the corresponding site and this might represent another possible layer of regulation (Stein et al., 1998; Stein et al., 1996).

In addition to the ephrin ligands, certain peptides can also induce forward signalling. For example, the YSA (YSAYPDSVPMMS) and to a lesser extent the SWL (SWLAYPGAVSYR) peptides compete with ephrin ligands by occupying their EphA2 interaction sites and cause EphA2 activation by inducing phosphorylation on its tyrosine residues. These monomeric peptides can also induce forward signalling. However, this fashion of activating the EphA2 receptor might be similar to the one

elicited by using soluble monomeric and unclustered ephrin-A1, although at this time it was thought that clustered EphA2 receptors are required for successful activation of the EphA2 receptor. Furthermore, there are also peptides known to bind to the EphA4, EphA5, EphA7, EphB1, EphB2 and EphB4. However, they are not able to cause activation of the respective receptor, but rather have an antagonistic effect (Noberini et al., 2012).

1.1.3. Ligand-independent functions of Eph receptors

The Eph receptors also possess the ability to facilitate signalling in the absence of phospho-tyrosine-mediated interactions (Fig. 2a). For example, ligand-independent signalling caused by phosphorylated Ser^{897} in the SAM domain of EphA2 by Akt promoted migration in U373 glioma cells (Miao et al., 2009). However, a recent study suggests that p90 ribosomal S6 kinases (RSKs) are responsible for Ser^{897} phosphorylation on EphA2 without any involvement of Akt. It was further proposed that Ser^{897} phosphorylation on EphA2 is connected to ligand-independent signalling, malignancy, migration and invasion (Zhou et al., 2015).

In contrast, the activation of EphA2 by its ligands and subsequent phosphorylation on tyrosine residues is associated with inhibition of migration in MDA-MB-231 cells, a malignant human breast cancer cell line (Shaw et al., 2014). In addition, activation of EphA2 by its ligands inhibits Akt and is thought to regulate Akt via a serine/threonine phosphatase (Yang et al., 2011) (Fig. 2b). Furthermore, kinase-independent functions exist for certain Eph receptors as they are involved in integrin-mediated cell adhesion without the requirement of kinase activity (Gu and Park, 2001; Matsuoka et al., 2005)

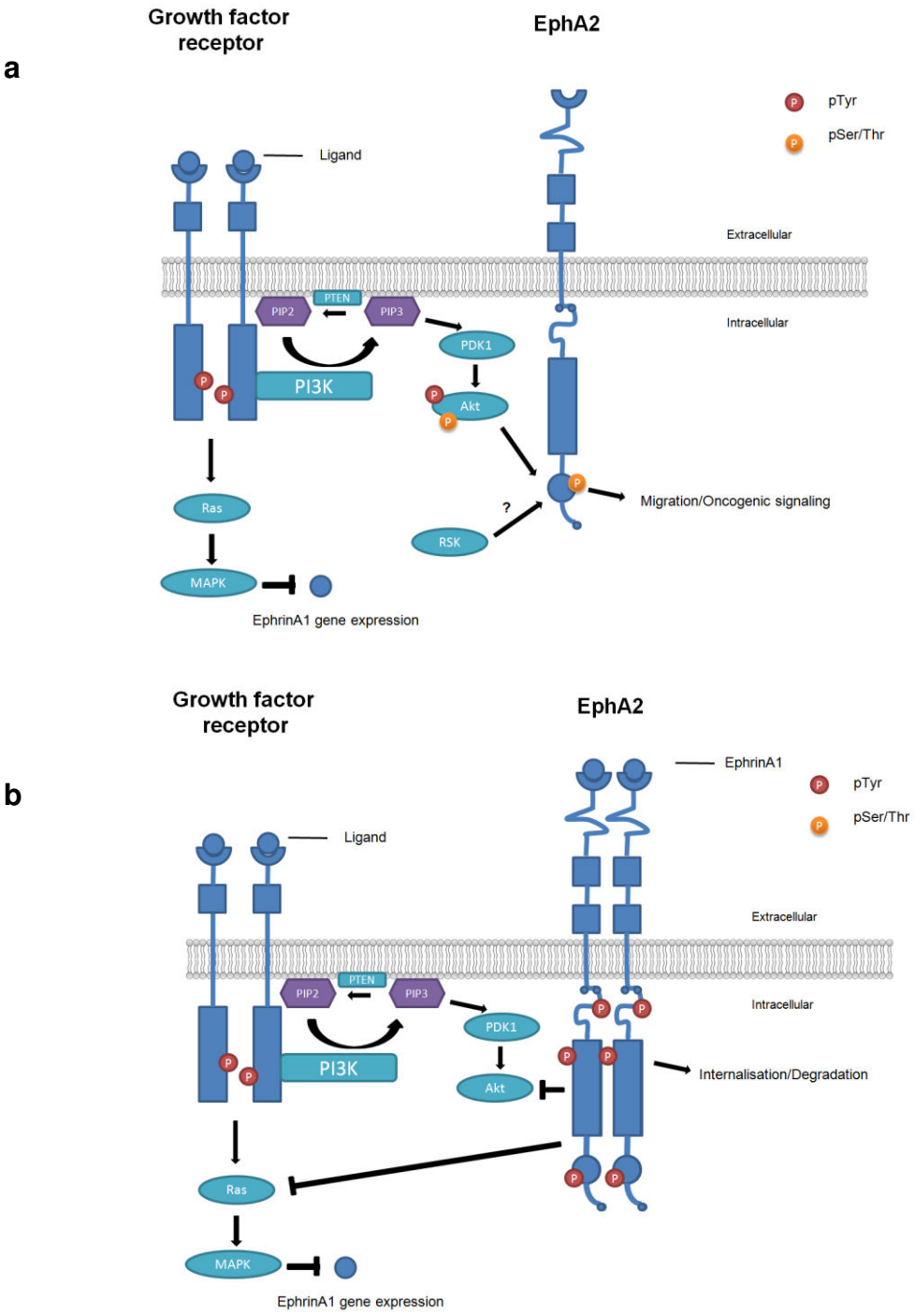

Figure 2: Current view of EphA2 signalling and its effect on Akt and HRas/Erk signalling **(a)** Ligand-independent signalling facilitated by EphA2; Growth factor receptor activation leads to the activation of Akt which establishes pSer^{897} on EphA2; pSer^{897} on EphA2 is associated with migration of malignant cells and promotion of oncogenic signalling; p90 ribosomal S6 kinase (RSK) also might be responsible for establishing pSer^{897} on EphA2 **(b)** Ligand-mediated signalling facilitated by EphA2; Binding of ligands on EphA2 leads to formation of a tetrameric signalling unit consisting of four Eph receptors and four ephrin ligands causing cross-phosphorylation of tyrosine residues on the Eph receptors and inhibition of Akt and Ras; MAPK, mitogen-activated protein kinases; PI3K,phosphatidylinositol-3-kinase; PTEN, Phosphatase and tensin homolog; PDK1, 3-phosphoinositide-dependent protein kinase-1

1.1.4. *Cellular effects after activation of Eph receptors*

Activation of the Eph receptors by ephrins can cause internalisation of the signalling complex by an endocytic pathway, in either the receptor or the ligand-expressing cell together with their surrounding plasma membranes, giving rise to internalized vesicles with double membranes (Pasquale, 2005). A disintegrin and metalloproteinase domain-containing protein 10 (ADAM10) cleaves ephrins from the cell surface. Trans-endocytosis occurs through a clathrin-mediated mechanism (Boyd et al., 2014). This results in degradation and removal of the signalling complex from the plasma membrane (Pasquale, 2010). Alternatively, interaction can also be terminated by cleavage of the Eph receptor or ephrin ligand extracellular domains. In the case of EphB2-ephrinB2 interaction it was shown that matrix metalloproteinase-2 (MMP-2) and MMP-9 can mediate cleavage in the ectodomain of EphB2, regulating repulsive responses in HEK293 cells (Lin et al., 2008). Kuzbanian, another metalloproteinase, was shown to bind to ephrin-A2 and to regulate ephrin-A2 mediated axon repulsion (Hattori et al., 2000). Furthermore, after cleavage of the extracellular domain, ɣ-secretase-mediated cleavage in the intracellular domains of Eph receptors or ephrins can occur, leading to distinctive signals (Georgakopoulos et al., 2006; Litterst et al., 2007; Tanaka et al., 2007).

Using ephrin-A1 that is displayed at a synthetic supported lipid membrane, a recent study could mimic certain aspects of the EphA2-ephrin-A1 trans-endocytosis occurring in living MDA-MB-231 cells. They could show that at sites of EphA2-ephrinA1 interactions ADAM10, clathrin and dynamin are recruited, proteins that are involved in endocytosis. Furthermore, they reported an actin bundle around sites of EphA2-ephrinA1 interactions. By restricting the lateral movement of ephrin-A1 through patterning in a supported lipid membrane they could show a decrease in endocytosed vesicles containing ephrin-A1. They conclude that there might be a threshold of EphA2-ephrinA1 clusters that is required for successful endocytosis and that restriction of the spatial movement of EphA2-ephrinA1 interactions regulate trans-endocytosis (Greene et al., 2014).

However, under certain cellular circumstances the Eph-ephrin signalling complex is localized at sites of cell-cell contact for a prolonged time. In the case of EphA2-ephrin-A1 interaction, E-cadherin promotes localization at epithelial cell junctions and reinforces and prolongs the signalling capacity of the complex (Zantek et al., 1999). Moreover, E-cadherin was shown to be regulating the expression of several Eph receptors and ephrins in embryonic stem (ES) cells (Orsulic and Kemler, 2000). In addition, recruitment of ADAM 19 was described to block internalisation of EphA4-ephrin-A5 at neuromuscular junctions despite its metalloproteinase activity (Yumoto et al., 2008).

LMW-PTP is thought to be an obstacle for initial events of tyrosine-phosphorylation on EphA2 in cases when enough ligand is expressed in the opposing cell to cause activation of EphA2 (Kikawa et al., 2002). Additionally, Eph receptor tyrosine phosphorylation is controlled by protein tyrosine phosphatase receptor type O (PTP-RO) (Shintani et al., 2006) and protein tyrosine phosphatase 1B (PTP1B) (Nievergall et al., 2010).

Forward signalling of the Eph receptors involves regulation of cytoskeletal dynamics and morphology of the corresponding cell (Fig. 3). In neurons, stimulation of EphA receptors with ephrins activate tuberous sclerosis complex 2 (TSC2) which leads to inactivation of Ras homolog enriched in brain (Rheb) (Nie et al., 2010). Activation of ephexin mediated by EphA gives rise to active ras homolog gene family, member A (RhoA) (Shamah et al., 2001). In both cases, these mechanisms result in neuron retraction and repulsion (Pasquale, 2010). Chimaerin was identified in neurons to be part of EphA4 forward signalling and to inhibit Ras-related C3 botulinum toxin substrate 1 (Rac1), thereby also mediating growth cone collapse (Iwasato et al., 2007). In the context of EphA2-ephrin-A1 signalling, reactive oxygen species (ROS) were proposed to regulate Rho activity involving LMW-PTP and p190RhoGAP (Buricchi et al., 2007). Alternatively, Rho activity was also suggested to be regulated through EphA2 by involving Src kinase instead of ROS, resulting in destabilisation of adherens junctions (Fang et al., 2008).

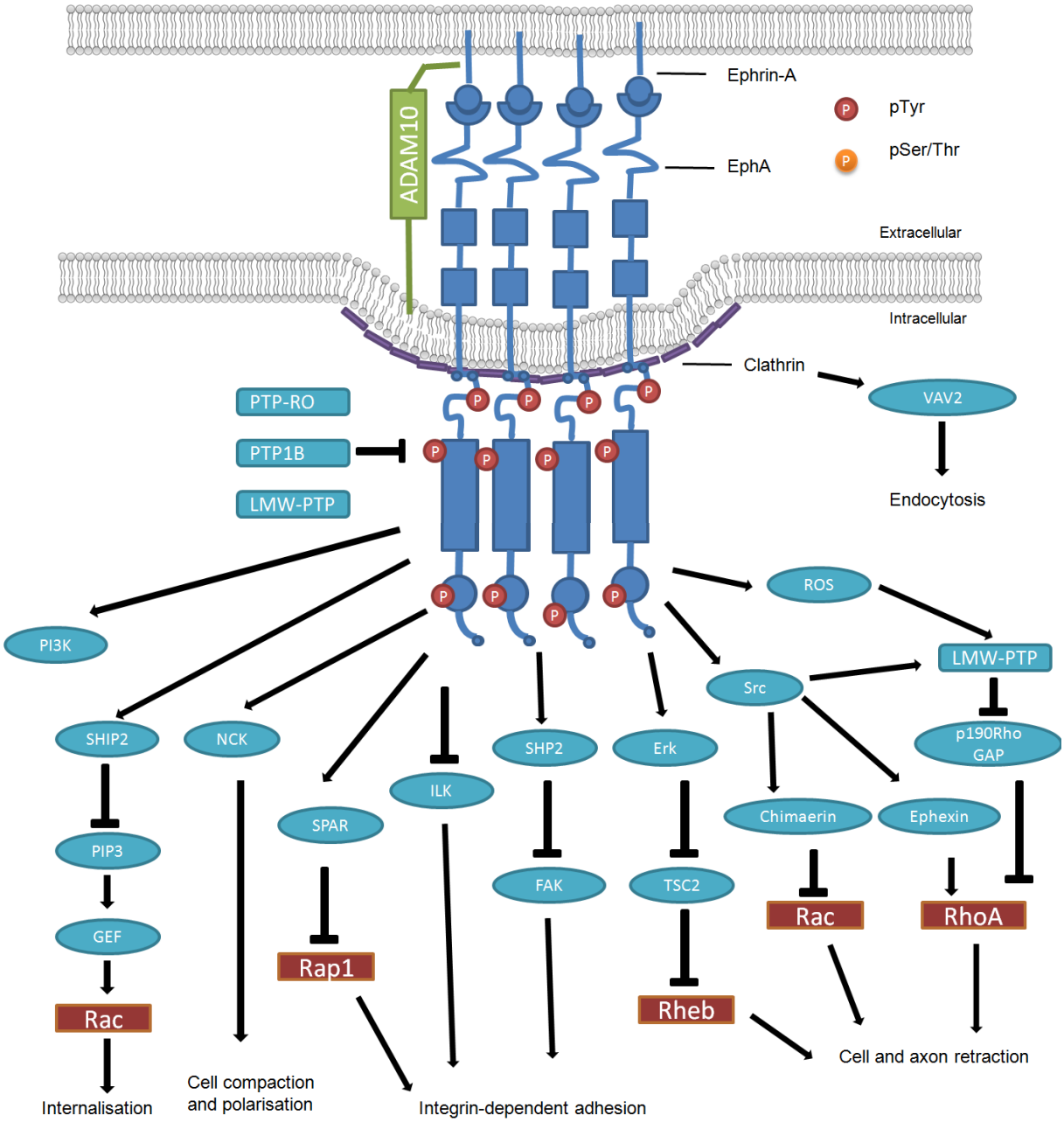

Figure 3: Signalling concepts that involve EphA and the actin cytoskeleton, migration and adhesion of cells. A disintegrin and metalloproteinase domain-containing protein 10 (ADAM10) cleaves ephrinA form opposing cell membranes and enables further endocytosis of the signalling complex; Endocytosis involves clathrin, dynamin and VAV2 GEFs. In neurons, signalling mediated by TSC2, chimaerin and ephexin results in characteristic repulsive effects. Inactivation of p190RhoGAP by low molecular weight tyrosine phosphatase (LMW-PTP) results in ras homolog gene family, member A (RhoA) activation. Dephosphorylation of focal adhesion kinase (FAK), signalling by spine-associated RapGAP (SPAR) and inactivation of integrin-linked kinase (ILK) lead to integrin-dependent adhesion. Activation of noncatalytic region of tyrosine kinase 1 (Nck1) results in cell compaction and polarisation. Recruitment of SH2-containing inositol phosphatase 2 (SHIP2) leads to inhibition of internalisation of the signalling complex. EphA2 can interact with the p85 subunit of PI3K and stimulate its activity after ligand binding. Rheb, Ras homolog enriched in brain; Rac1, Ras-related C3 botulinum toxin substrate 1; ROS, reactive oxygen species; Rap1, Ras-proximate-1 or Ras-related protein 1

Focal adhesion kinase (FAK) associates with EphA2 and upon ligand stimulation, Src-homology 2 domain-containing phosphatase 2 (SHP2) inactivates focal FAK, leading to the inhibition of integrin-dependent adhesion (Miao et al., 2000; Pasquale, 2005). Inhibition of Ras-proximate-1 or Ras-related protein 1 (Rap1) occurs through spine-associated RapGAP (SPAR) (Richter et al., 2007). Activation of the EphA1 receptor causes a decrease in the integrin-linked kinase (ILK) activity (Yamazaki et al., 2009).

Non-catalytic region of tyrosine kinase 1 (Nck1) can bind to ligand-stimulated EphA2 and mediates cell compaction and polarisation in Madin-Darby kidney cells (Miura et al., 2009). Despite the finding that Akt is inhibited by EphA2 after stimulation with its ligand (Miao et al., 2009), the subunit p85 of PI3K can directly bind Eph and stimulation with ligands increases the activity of PI3K (Pandey et al., 1994).

Activation of the receptor and endocytosis involves VAV2 GEFs (Pitulescu and Adams, 2010). SH2-containing inositol phosphatase 2 (SHIP2) is recruited to the SAM domain of EphA2 and leads to Rac1 inactivation and inhibition of EphA2 internalisation (Zhuang et al., 2007).

Pathways that are involved in EphB receptor-mediated forward signalling are Ras/Rho GTPases, ABL and mitogen-activated protein kinases (MAPKs) (Pitulescu and Adams, 2010; Pasquale, 2008; Jørgensen et al., 2009; Pasquale, 2010).

Eph receptors are involved in multiple cellular functions in a normal state and are predominantly expressed during development but are also important in adult tissue for regeneration and organ structure maintenance (Boyd et al., 2014). Eph/ephrin signalling is implicated in axon guidance, tissue patterning, angiogenesis, cell survival and adhesion (Nikolov et al., 2013; Wilkinson, 2001).

1.1.5. *Ephrin-A1 induced signalling mediated by EphA2 in the context of cancer*

Dysregulation of the Eph/ephrin pathway has been linked to various diseases including cancer. For example, the dysregulated Eph/ephrin pathway possesses both tumour-suppressing and tumour-promoting qualities and both elevated and decreased levels of various Eph receptors and ephrins are linked to cancer, indicating the complexity of this particular signalling pathway (Pasquale, 2010).

Overexpression of EphA2 and association with malignancy and poor clinical prognosis was confirmed in a variety of different tumours, including melanomas, ovarian, bladder, gastric and cervical cancer (Easty et al., 1995; Thaker et al., 2004; Abraham et al., 2006; Yuan et al., 2009; Holm et al., 2008). In breast cancer cell lines the expression of ephrin-A1 is decreased, whereas an increase in expression of EphA2 is reported (Fox and Kandpal, 2004). This is associated with a higher potential of invasiveness of these cells. This pattern can also be observed in glioblastoma multiforme (GBM) tumour specimen (Wykosky et al., 2005). In breast cancer cell lines this differential expression pattern is suggested to be regulated by the MAPK pathway, which was shown to inhibit ephrin-A1 expression in EphA2 expressing cells (Macrae et al., 2005) (Fig. 2).

Studies have shown that despite overexpression of EphA2 in malignant cells, the amount of tyrosine-phosphorylated EphA2 is quite low (Himanen et al., 2007). Evidence suggests that this is partly caused by LMW-PTP leading to a reduction of tyrosine-phosphorylated EphA2 in tumour cells (Kikawa et al., 2002).

The ability of solid tumours to promote the growth of new blood vessels depicts an important feature to ensure the delivery of nutritional factors and is a gateway for dissemination and metastasis. Activation of EphA2 by endothelial cells with its ligand ephrinA1 was shown to maximize the angiogenic effect of vascular endothelial growth factors (VEGFs). Therefore, EphA2 might represent a novel target for

intervention of neovascularisation of solid tumours (Pandey et al., 1995; Cheng et al., 2002).

The current view indicates that EphA2 activation by its ligands leads to inhibition of the HRas-Erk pathway (Fig. 2b; Fig. 4). EphA2's role in the pathway also involves a negative feedback loop, as Raf increases EphA2 levels and EphA2 stimulation attenuates growth factor induced activation of the MAPK pathway (Miao et al., 2001). However, in MDA-MB-231 cells the attenuation of the MAPK pathway could not be observed (Macrae et al., 2005). This is due to a mutation in B-Raf and an activated allele of KRAS in this particular cell line, leading to insensitivity of the pathway towards upstream signals (Wilhelm et al., 2004; Ogata et al., 2001; Kozma et al., 1987). However, it has also been reported that the MAPK pathway is activated and EphA2 mRNA levels are elevated in MDA-MB-231 cells after stimulation with IgG-clustered ephrin-A1 (Pratt and Kinch, 2003). A mechanism that mediates activation of the MAPK pathway is thought to involve Src homology 2 domain containing (SHC) transforming protein and growth factor receptor-bound protein 2 (GRB2) (Pratt and Kinch, 2002).

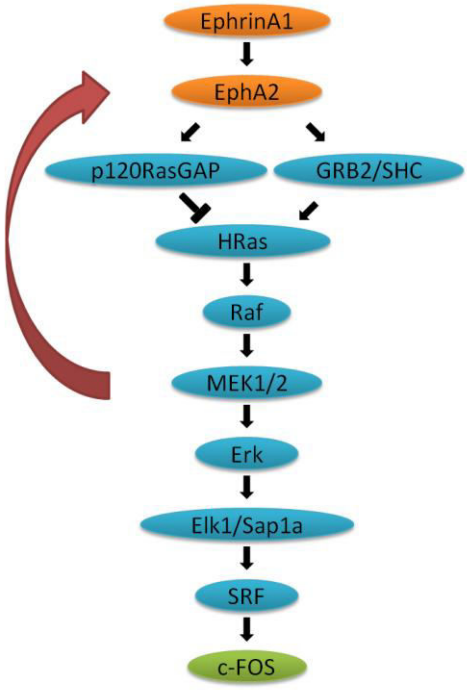

Figure 4: Negative feedback-loop of EphA2 forward signalling and HRas-Erk; Stimulation of the HRas-Erk pathway by Src homology 2 domain containing (SHC) transforming protein and growth factor receptor-bound protein 2 (GRB2), black arrows indicate direct regulation; red arrow indicates regulation on an mRNA level

1.2. DNA origami – Nanocalipers

As mentioned above, activation of Eph receptors can be achieved by membrane bound or artificially-clustered ephrins. Artificial clustering is performed by mixing ephrin-A5-Fc to IgG antibodies in a certain ratio. Nanoscale distribution of ephrin-A5 ligands plays a role in the invasion capacity of MDA-MB-231 cells (Shaw et al., 2014). As artificial clustering does not allow for precisely defining the distance and distribution of clustered ligands, there is a need for a tool that allows for exactly determining the nano-spatial distribution of ligands. Recently, a method was established using DNA origami that provides for this need (Shaw et al., 2014).

The principle of DNA origami is based on hybridising a long ssDNA scaffold with many short ssDNA fragments, so-called staples thereby forming a distinct 3D DNA structure (Fig. 5a). This requires precise planning and computational modelling of the prospective DNA origami construct in order to obtain a stable and well-folded structure. To define the nano-spatial distribution of ligands, DNA origami structures termed nanocalipers are used. Nanocalipers consist of a tubular structure and can be produced in a way to possess ssDNA protrusions at defined positions. Ligands conjugated to a complementary ssDNA fragment can be hybridised to these protrusions. This allows for the exact identification of their position on the nanocaliper. As the positions of the ligands on the nanocalipers are known, one can specifically control the distance between each ligand on the structure (Fig. 5b,c). Furthermore, this method ensures the nanospatial distribution of the ligands independent of the concentration of nanocalipers (Shaw et al., 2014).

In addition, recent advances in the field of DNA origami now allow for assembly of complex arbitrary polyhedral meshes (Benson et al., 2015). This might allow for the formation of more complex ligand patterns in future experiments.

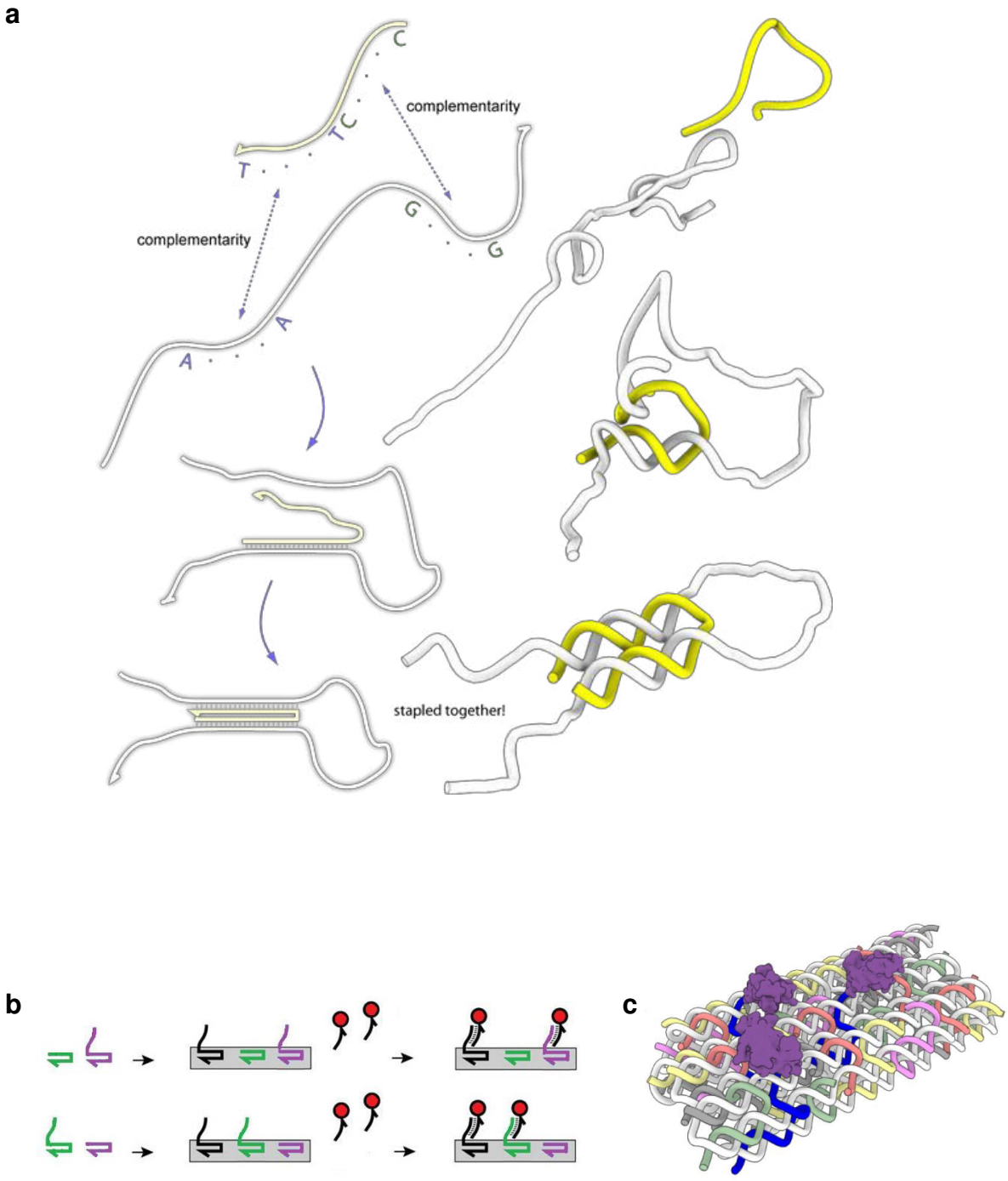

Figure 5: (a) Principle of DNA-origami folding resulting in complex 3-D structures (used with permission from Björn Högberg) **(b,c)** Schematic of the ephrin-A5 nanocalipers; Position of protruding oligos are known by design and ligands conjugated to a complementary ssDNA fragment can be hybridised at these defined positions (Fig. 5b adapted from Alan Shaw et al., 2014; Fig. 5c used with permission from Björn Högberg)

1.3. Proximity ligation assay

Proximity ligation assay (PLA) is a method that allows for the detection of proteins, protein-modifications and protein interactions (Söderberg et al., 2006; Weibrecht et al., 2010). The principle is to use two primary antibodies raised in different species to recognize the desired antigens of interest. Two secondary antibodies conjugated to a short ssDNA fragment then bind the primary antibodies. Only if the secondary antibodies are in close proximity (<40 nm), the ssDNA fragments can bind two connector oligos that are partially complementary to both ssDNA fragments, resulting in a circle of connector oligos. Subsequently, these are ligated and continuous rolling circle amplification is carried out. Fluorescently labelled probes are added to the amplified DNA, resulting in a quantifiable dot (Fig. 6a-e).

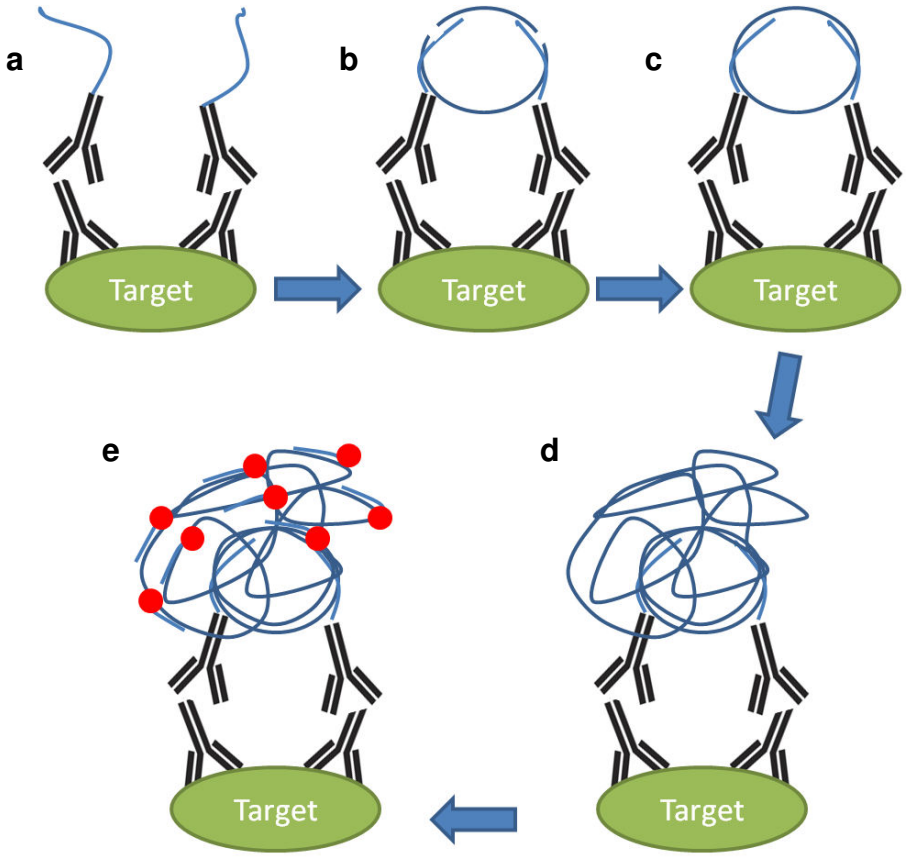

Figure 6: Principle of PLA **(a)** Primary and secondary antibodies bind to a target; Secondary antibodies are conjugated to a short ssDNA oligo. **(b)** Two connector oligos bind to the ssDNA oligos if they are in close proximity **(c)** Ligation is carried out to yield a complete circular DNA structure **(d)** Rolling circle amplification to amplify DNA **(e)** Hybridize fluorescently labelled ssDNA probes to amplified DNA

2. Project outline

Co-expression of multiple different Eph receptors and ephrins on one cell and co-clustering and crosstalk with various signalling pathways make signalling mediated by these receptor-ligand pairs particularly complex. Ultimately, the cellular response is often cell type and tissue specific (Boyd et al., 2014). As previously shown, another layer of complexity is created by the regulation of the nano-spatial distribution of the ephrin ligands that are presented to neighbouring cells, which can elicit distinct cellular outcomes (Shaw et al., 2014). This contributes to the phenomena of the apparent dichotomous effects mediated by Eph/ephrin signalling.

MDA-MB-231 cells were reported to show decreased cell invasiveness when presented with nanocalipers bearing ephrin-A5 ligands that are spaced 40 nm or 100 nm apart. The ephrin-A5 ligands that were spaced 40 nm apart yielded a larger reduction of the cell invasion properties of MDA-MB-231 cells. Therefore, a nano-spatial distribution of these ligands clearly seems to play a role in this context (Shaw et al., 2014). Furthermore, the EphA2 receptor is highly overexpressed in this cell line, making it ideal for studying the role of this particular Eph receptor in the context of cell invasion (Zelinski et al., 2001). In addition, EphA2 in MDA-MB-231 cells is not phosphorylated on its phospho-tyrosine residues under basal conditions (Pratt and Kinch, 2003), but the Ser^{897} residue is constantly phosphorylated (Zhou et al., 2015). Nevertheless, EphA2 in MDA-MB-231 cells retains its enzymatic ability and shows kinase activity when artificial clustering of EphA2 receptors is induced (Zantek et al., 1999).

As a next step, we chose to investigate the intracellular effects leading to this differential response. The final goal is to perform RNA-seq and to uncover the initial response on the transcriptome of MDA-MB-231 cells when exposed to different ephrin-A5 nanocalipers.

In order to achieve this goal, a system meeting several requirements needs to be established. These requirements are to show consistent and prominent activation of the EphA2 receptor, activation of downstream target proteins and stable gene expression and activation of known target genes. Fabrication of nanocalipers is still very time-consuming and elaborate. Therefore, the initial experiments were performed with homo-dimeric recombinant human ephrin-A5 fused to Fc of human IgG and clustering was achieved by adding goat anti-human IgG, which is Fc fragment specific. This fashion of clustering ephrin-A5 dimers is hereafter referred to as IgG-clustered ephrin-A5. The molar ratio of IgG compared to ephrin-A5 is 6.4:1. Hence, all the ephrin-A5 dimers should be bound to IgG. Furthermore, a comparison of monomeric, dimeric and IgG-clustered ephrin-A5 showed that IgG-clustered ephrin-A5 is able to activate the EphA2 receptor more efficiently 15 min after stimulation than the other forms (Shaw et. al; 2014). As we are seeking for high activation of the EphA2 receptor in response to stimulation with ligands and intra-cellular effects connected to activation, IgG-clustered ephrin-A5 was used in the initial optimisation experiments. In addition, homo-dimeric recombinant human ephrin-A5 is also bound to the nanocalipers in varying distances. Using nanocalipers, it is ensured that all the ephrin-A5 dimers are bound to the DNA origami structure.

Previous experiments from Shaw *et. al* (2014), on which this project is based on, were conducted on micropatterns that only have specific islands on which cells can attach. Therefore, they are both restricted in their movement and it is ensured that the cells cannot touch each other. This prevents activation of the EphA2 receptor originating from ephrin-As that are expressed on neighbouring cells. To circumvent the excessive use and need of micropatterns for the optimisation of the system and to investigate also EphA2 receptor activation in an alternative way, cells were plated on coverslips coated with fibronectin instead. This allows the cells to spread out, keep its native shape and does not restrict the cells in their movement. Cells plated on coverslips have the ability to touch each other and to facilitate signalling even in the absence of treatment. To limit these events, we were plating cells in a very low density, trying to avoid having cells touch each other. As the use of micropatterns represents a very controlled and standardized manner of handling cells, the idea is to also perform the final RNA-seq experiments with cells that were seeded on micropatterns.

Initially, the behaviour of MDA-MB-231 cells and extent of EphA2 receptor activation on both micropatterns and coverslips were compared. In addition, cells plated on coverslips were also treated with nanocalipers bearing ephrin-A5 ligands that were differentially spaced apart and activation dynamics of the EphA2 receptor was assessed.

To investigate the intracellular effects of MDA-MB-231 cells after treatment with ephrin-A5, we chose the HRas-Erk pathway as readout for the stability of our system. Target proteins were Erk1 and Erk2 and their respective phosphorylated form, Erk1 (pT202/pY204) and Erk2 (pT185/pY187), hereafter referred to as Erk and pErk. Target genes investigated in connection with the HRas-Erk pathway were c-FOS and ELK1.

A former lab member observed changes in the genes CTNNA1, HK2, IRAK4 and KSR1 in a preliminary RNA-seq experiment in which MDA-MB-231 cells were stimulated with IgG-clustered ephrin-A5. Therefore, we also investigated expression profiles of these genes. Another pathway we examined was the PI3K/Akt pathway. Targets genes that were investigated and are all related to this pathway are RUNX2, FOXP1, PALLD and CCDC88A (Chin and Toker, 2010; Enomoto et al., 2006; Halacli and Dogan, 2015; Tandon et al., 2014).

Stimulation or effects observed regarding the tested target genes can be used as a reference for the final RNA-seq experiments. Moreover, the data obtained will be used to evaluate the optimal time points after stimulation with IgG-clustered ephrin-A5 for extraction of RNA of stimulated cells for the RNA-seq experiments.

3. Materials and Methods

3.1. Cell Culture

MDA-MB-231 cells (ATCC – HTB26D) were cultured at 37 ° C, 5 % CO2 in Dulbecco's modified Eagle medium + GlutaMAX™ (DMEM + GlutaMAX™) (Gibco Life Technologies REF 31966-021) supplemented with 10 % fetal bovine serum (FBS) (Gibco Life Technologies REF 10270-106) and 1 % penicillin/streptomycin (P/S) (Gibco Life Technologies REF 15140-122). Cells were grown until confluent and split every 2-3 days in a normal fashion using TrypLE™ Express (Gibco Life Technologies REF 12604-013). To perform PLA or pErk/Erk staining experiments, cells were grown in a 24-well plate on a coverslip (VWR – Cat. No. 631-0169) coated with fibronectin (Sigma-Aldrich, F1141 – Fibronectin from bovine plasma) in a density of 10,000 cells/well or in a 4-well CYTOO chamber (CYTOO REF 30-011) on a micropatterned glass slide (CYTOO REF 10-001-00-18) coated with fibronectin in a density of 10,000 cells/well. The micropatterned islands were disc-shaped and had a diameter of about 30 µm. Cells were allowed to attach in DMEM + GlutaMAX™ supplemented with 10 % FBS and 1 % P/S for 1 h before unattached cells were washed off and the media was replaced with DMEM + GlutaMAX™ supplemented with 1 % P/S. To perform RNA isolation cells were grown in a 24-well plate for c-FOS and ELK1 experiments in a density of 10,000 cell/well. For the other genes tested cells were grown in a 96-well plate in a density of 2,000 cells/well. If cells were used for subsequent RT-qPCR experiments only the wells were coated with fibronectin. Coating was performed with 40 µg/ml fibronectin for 30 min at room temperature.

3.2. Stimulation of Eph receptors

Cells were serum starved in DMEM + GlutaMAX™ supplemented with 1 % penicillin/streptomycin for 1 h or 24 h prior to stimulation. Recombinant human ephrin-A5-Fc chimera (RnD Systems – REF 374-EA) were preclustered using polyclonal AffiniPure Goat Anti-Human IgG (Fcy-Fragment specific, Jackson Immunoresearch REF 109-005-008), hereafter referred to as IgG-clustered ephrin-

A5. This was performed at a ratio of 1:10 (ephrin-A5-Fc and IgG antibodies, respectively) mixed in DMEM + GlutaMAX™ supplemented with 1 % penicillin/streptomycin for 15 min at room temperature. Stimulation was carried out at a final concentration of either 0.5 µg/ml or 1 µg/ml of ephrin-A5-Fc (clustered with 5 µg/ml or 10 µg/ml of IgG antibodies final, respectively). Stimulation for experiments with nanocalipers (generously provided by the lab of Björn Högberg, Karolinska Institutet) was carried out at a final concentration of 20 nM ephrin-A5-Fc, corresponding to 1 µg/ml, conjugated to DNA nanocalipers. Nanocalipers used were bearing ephrin-A5 ligands that are spaced 0 nm (NC0), 40 nm (NC40) or 100 nm (NC100) apart. Controls were only treated with the corresponding concentration of IgG antibodies or empty nanocalipers (NCempty).

For the initial PLA and Erk staining optimisation experiments (Fig. 7a-d; Fig. 8; Fig.9a-h; Fig. 10a,b) the 0 min time point was treated with IgG antibodies alone together with the longest time point performed and data was normalized over this 0 min time point. For subsequent PLA experiments and the RT-qPCRs, a control treated condition for each time point was carried out separately and the 0 min time point was untreated. Cells on the coverslip in the initial PLA experiments (Fig. 7a-d; Fig. 8) were treated in a 24 well plate with the corresponding concentration of IgG-clustered ephrin-A5 or IgG alone. Cells in subsequent PLA experiments were treated by inverting the coverslip on a droplet (55 µl) of solution containing the corresponding concentration of IgG-clustered ephrin-A5, IgG alone or nanocalipers. Data of the nanocaliper PLA experiments (Fig. 14; Fig. 15) was normalized over the respective 30 min control treated condition.

3.3. Proximity Ligation Assay

Unless stated otherwise all the reagents for PLA were obtained from Sigma-Aldrich (DUO92007-100RXN, DUO92004-30RXN, DUO92002-100RXN). Coverslips were incubated with Duolink II Blocking Solution, the respective antibodies and dyes in a humidity chamber. A droplet of the required solution was placed on parafilm and the coverslip was placed there in such a fashion that the cells face the solution. After the

amplification step, samples were kept under light-sensitive conditions. Wash steps were carried out with 500 µl in a 24-well plate.

After stimulation with clustered ephrin-A5-Fc or nanocalipers or the respective controls, the cells were washed once with cold Dulbecco's Phosphate-Buffered Saline (Gibco Life Technologies REF 14190-094). Fixation was done with 10 % formalin for 20 min at room temperature. Subsequently, cells were washed three times for 5 min each with PBS in gentle agitation. Permeabilisation was performed by washing the samples with PBS/0.1 % Triton X-100 three times for 10 min followed by three washes for 5 min with TBS-0.1 % Tween 20 and one wash with PBS. Samples were incubated with one drop of Duolink II Blocking Solution in a humidity chamber for one hour at 37 ° C, followed by one wash with PBS. Primary antibody incubation was carried out overnight at 4 ° C. The α-pTyr antibody (Abcam, cat. no. ab9319) was used in a dilution of 1:1200 and the α-EphA2 antibody (Millipore, clone D7, cat. no. 05-480) was used in a dilution of 1:1500. Dilutions of the primary antibodies were done in Duolink II Antibody (1x) diluent. The next day, samples were washed three times with Duolink Wash Buffer A for 10 minutes each. Subsequently, samples were incubated with the Duolink II α-Mouse MINUS and the Duolink II α-Rabbit PLUS in a dilution of 1:80 for 60 min at 37 ° C. Dilutions of the secondary antibodies were made in Duolink II Antibody (1x) diluent. Again three washes with Duolink Wash Buffer A for 10 minutes each were performed. Ligation stock (5x) was diluted 1:5 and ligase was diluted 1:80 in water. Ligation was carried out for 30 min at 37 ° C followed by two washes with Duolink Wash Buffer A for 2 min. Amplification stock (5x) was diluted 1:5 and polymerase was diluted 1:160 in water. Amplification was performed for 60 min at 37 ° C followed by two washes with Duolink Wash Buffer B for 10 minutes each and one wash with PBS for 5 min.

Then either Alexa Fluor 488 phalloidin (Life Technologies – cat. no. A12379) staining or Anti-Erk1 (pT202/pY204) + Erk2 (pT185/pY187) (Abcam, cat. no. ab76165) staining was carried out. Alexa Fluor 488 phalloidin (Life Technologies REF A12379) staining was performed in a dilution of 1:100 in PBS for 30 min at room temperature.

In case Anti-Erk1 (pT202/pY204) + Erk2 (pT185/pY187) staining was performed, samples were again fixed with 10 % formalin for 15 min at 37 ° C, followed by two quick washes with PHEM buffer and two washes with PBS for 5 min. Blocking was carried out with PBS + 3 % BSA (Sigma-Aldrich A7906) for 30 min at room temperature. Anti-Erk1 (pT202/pY204) + Erk2 (pT185/pY187) antibody was diluted 1:300 in PBS + 1 % BSA and samples were incubated two hours at room temperature. Subsequently, samples were washed three times with cold PBS + 1 % BSA for 5 min each followed by another three quick washes with cold PBS + 1 % BSA. The secondary antibody Alexa Fluor 488 (Abcam, cat. no. ab150077) was diluted 1:1000 in PBS + 1 % BSA and incubated for one hour at room temperature.

In both cases, samples were subsequently washed once with PBS for 5 min and then stained with 4′,6-diamidino-2-phenylindole (DAPI – Sigma-Aldrich REF D9542) in a dilution of 1:750 in PBS for 10 min at room temperature. Samples were washed twice with PBS for 5 min each. Coverslip and micropattern was mounted using 6 µl and 20 µl Mowiol, respectively.

Images for quantification of PLA signal were obtained using the Zeiss Cell Observer fluorescent microscope. Only single cells, which were not touching, were imaged. Images were acquired with the 40x objective in a z-stack mode. 8 images of 3 µm thick slices per cell were obtained for the initial optimization experiments (Fig. 7a,b) or the 20 images of 1 µm thick slices per cell were obtained for subsequent PLA experiments. The middle z-stack is in the focal plane; therefore ensuring to acquire images throughout the cell. Per condition, at least 20 cells were imaged and analysed. Analysis was carried out using ImageJ. Images were hyperstacked with maximum intensity z-projection, region covered by cell was estimated using the Alexa Fluor 488 phalloidin or the Anti-Erk1 (pT202/pY204) + Erk2 (pT185/pY187) staining and dots within this region were counted after a simple background reduction. Further analysis and visualisation of data was done using Prism software (GraphPad).

3.4. Immunocytochemistry (ICC)

Coverslips were incubated with the respective antibodies and dyes in a humidity chamber. A droplet of the required solution was placed on parafilm and the coverslip was placed there in such a fashion that the cells face the solution. After incubation with secondary antibodies, samples were kept under light-sensitive conditions.

After stimulation with clustered ephrin-A5-Fc, the cells were washed once with cold Dulbecco's Phosphate-Buffered Saline. Fixation was done with 10 % formalin for 20 min at room temperature. Subsequently, cells were washed once for 5 min each with PBS in gentle agitation. Permeabilisation was performed by washing the samples with PBS/0.1 % Triton X-100 once times for 10 min followed by one wash with PBS. Samples were incubated with 3 % BSA (Sigma-Aldrich A7906) in PBS for one hour at 37 ° C followed by one wash with PBS. Primary antibody incubation was carried out for 1 h at 37 ° C. The Anti-Erk1 (pT202/pY204) + Erk2 (pT185/pY187) antibody (Abcam, cat. no. ab76165) was used in a dilution of 1:250 and the Anti-Erk1 + Erk2 antibody (Abcam, cat. no. ab54320) was used in a dilution of 1:300. Dilutions of the primary antibodies were made in 1 % BSA in PBS. Samples were washed three times with PBS for 5 minutes each. Subsequently, samples were incubated with the secondary antibodies for 1 h at 37 ° C. The Alexa Fluor 488 anti-Rabbit antibody (Abcam ab15007) was used in a dilution of 1:1000 and the Alexa Fluor 594 anti-Mouse antibody (Life Technologies A21203) was used in a dilution of 1:250. Dilutions of the secondary antibodies were done 1 % BSA in PBS. Samples were washed three times with PBS for 5 minutes each. Samples were subsequently stained with 4′,6-diamidino-2-phenylindole (DAPI – Sigma-Aldrich REF D9542) in a dilution of 1:750 in PBS for 10 min at room temperature. Samples were washed twice with PBS for 5 min each. Coverslip was mounted using 6 µl Mowiol.

Images for assessment of the intensity of Anti-Erk1 (pT202/pY204) + Erk2 (pT185/pY187) and the Anti-Erk1 + Erk2 stainings were obtained using the Zeiss Cell Observer fluorescent microscope. Images were acquired with the 40x objective in a z-stack mode. 20 images of 1 µm thick slices per cell were obtained, having the middle z-stack in the focal plane; therefore ensuring to acquire images throughout

the cell. Per condition, at least 20 cells were imaged and analysed. Analysis was carried out using ImageJ. Images were hyperstacked with sum slices z-projection, region covered by cell was estimated using the Anti-Erk1 (pT202/pY204) + Erk2 (pT185/pY187) staining. Intensities of both stainings were obtained and corrected total cell fluorescence (CTCF) was calculated. Formula used was: CTCF = Integrated Density - (Area of selected cell x Mean fluorescence of background readings). Further analysis and visualisation of data was done using Prism software (GraphPad).

3.5. RNA isolation and RT-qPCR

Testing the genes c-FOS and ELK1, the following experimental procedures were used: After stimulation with clustered ephrin-A5-Fc the cells were put on ice and washed once with cold Dulbecco's Phosphate-Buffered Saline. Subsequently, RNA was isolated using the Qiagen Rneasy® Micro Kit (cat. no. 74004) according to manufacturer's protocol. Briefly, for each well, 75 µl of RLT Buffer supplemented with 1:100 β-mercaptoethanol and 75 µl of 70 % ethanol were used. Concentration of the isolated RNA was determined by measuring with Nanodrop2000 and 50 ng of total RNA were reverse transcribed into cDNA using the High Capacity cDNA Reverse Transcription Kit (Applied Biosystems - Part No. 4368814) according to manufacturer's protocol using RNase Inhibitor (ThermoFisher – Cat. No. EO0381). RT-qPCR was performed using 5 ng of cDNA per reaction and the FastSYBR Green Mix (Applied Biosystems – Part No. 4385612).

Testing other genes, the following experimental procedures were used: After stimulation with clustered ephrin-A5-Fc the cells were put on ice and washed once with cold Dulbecco's Phosphate-Buffered Saline. Lysis, RT-reaction and qPCR were carried out using the Power SYBR® Green Cells-to-C_T™ Kit (Cat. No. 4402954) according to manufacturer's protocol. 55 µl of lysis-stop solution mix were pooled from two independent biological replicates before the subsequent RT reaction. 45 % of RT mix consisted of lysis-stop solution mix. 5 % of lysis volume from an individual experiment was used for each final qPCR run.

The following primer sequences were used:

Primer name	Primer sequence (5'-3')
CCDC88A_Fw	GGCAGAACATCCACTAGCAATA
CCDC88A_Rev	ATGGTCATGAAGCAGGCTAAA
CTNNA1_Fw	CAGGATCCAGGATGGACAAG
CTNNA1_Rev	TGCAGATGTTCAGCTGGT
ELK1_Fw	TTCTGGAGCACCCTGAGT
ELK1_Rev	CACGCTGATAGAAGGGATGTG
FOS_Fw	AGGAGGGAGCTGACTGATAC
FOS_Rev	CTTCTCCTTCAGCAGGTTGG
FOXP1_Fw	CCTACTGCACACCTCTCAATG
FOXP1_Rev	CGTATTGCGCTGGCTAAGT
HK2_Fw	GATTTCACCAAGCGTGGACTA
HK2_Rev	CAGGCAGTCACTCTCAATCTG
IRAK4_Fw	AAGCTTTGCGTGGAGAAATAAC
IRAK4_Rev	CTGAGGTTCACGGTGTTCAT
PALLD_Fw	CGGCTGGAATGTCGTGTATT
PALLD_Rev	CAGATGTAGCCGTGGTTGTC
KSR1_Fw	TGAGATTGTACGCGAGATGAC
KSR1_Rev	GCTTGCAGCTCATACCAAAC
RUNX2_Fw	CCACAAGGACAGAGTCAGATTAC
RUNX2_Rev	GGGTGGTAGAGTGGATGGA

3.6. Statistical analysis

For analysis in Figure 11a, we performed Wilcoxon matched-pairs signed rank test. D'Agostino's normality test could not be performed as the sample size (n) was too small. For data in Figure 13, *n* was too small to perform Wicoxon matched-pairs signed rank test, therefore we assumed Gaussian distribution and unpaired t-test was carried out.

4. Results

4.1. Stimulation with IgG-clustered ephrin-A5 causes tyrosine-phosphorylation of the EphA2 receptor

In order to quantify the extent of EphA2 receptor tyrosine-phosphorylation, we used the *in situ* proximity ligation assay (PLA). MDA-MB-231 cells were plated either on substrates with micropatterned fibronectin islands of defined size or on fibronectin-coated coverslips. Cells were serum starved for 1 h when plated on micropatterns or both 1 h and 24 h when plated on coverslips. We could observe the predicted increase in EphA2 receptor phosphorylation in the cells treated with IgG-clustered ephrin-A5. Cells that were serum starved for 1 h and plated on micropatterns show a rather consistent activation of 1.7-2.3 folds throughout the time points tested (Fig. 7a; Table 1). Cells that were serum starved for 1 h and plated on coverslips show a peak of activation at 15 min after treatment of 2.9 fold and the signal persists until 60 min and decreases to basal levels at 90 min (Fig. 7b; Table 1). In addition, the standard error in the experiments with coverslips is higher than in the experiments with micropatterns. In these experiments a concentration of 0.5 µg/ml of IgG-clustered ephrin-A5 was used for stimulation.

The most prominent phosphorylation of the EphA2 receptor was achieved if cells plated on coverslips were serum starved for 24 h and then treated with 1 µg/ml IgG-clustered ephrin-A5 (Fig. 7c,d). The peak of activation of 4.2 fold could be observed at 15 min after stimulation and decreased to 2.7 fold at 60 min (Table 1). In addition, MDA-MB-231 cells that were serum starved for 24 h were also treated with IgG alone at the time points tested (Fig. 8). IgG control treated samples did not show any stimulation if the raw data is compared to 1 µg/ml IgG clustered ephrin-A5 treated conditions. This IgG control experiment was done together with one of the treatment experiments showing higher background in the 0 min time point. The 0 min time point showed exceptionally low signal in the IgG control treated condition. Therefore, normalization over the 0 min time point would imply that stimulation of the EphA2 receptor occurs when IgG alone is presented to the cells, although the raw data shows clearly that this is not the case.

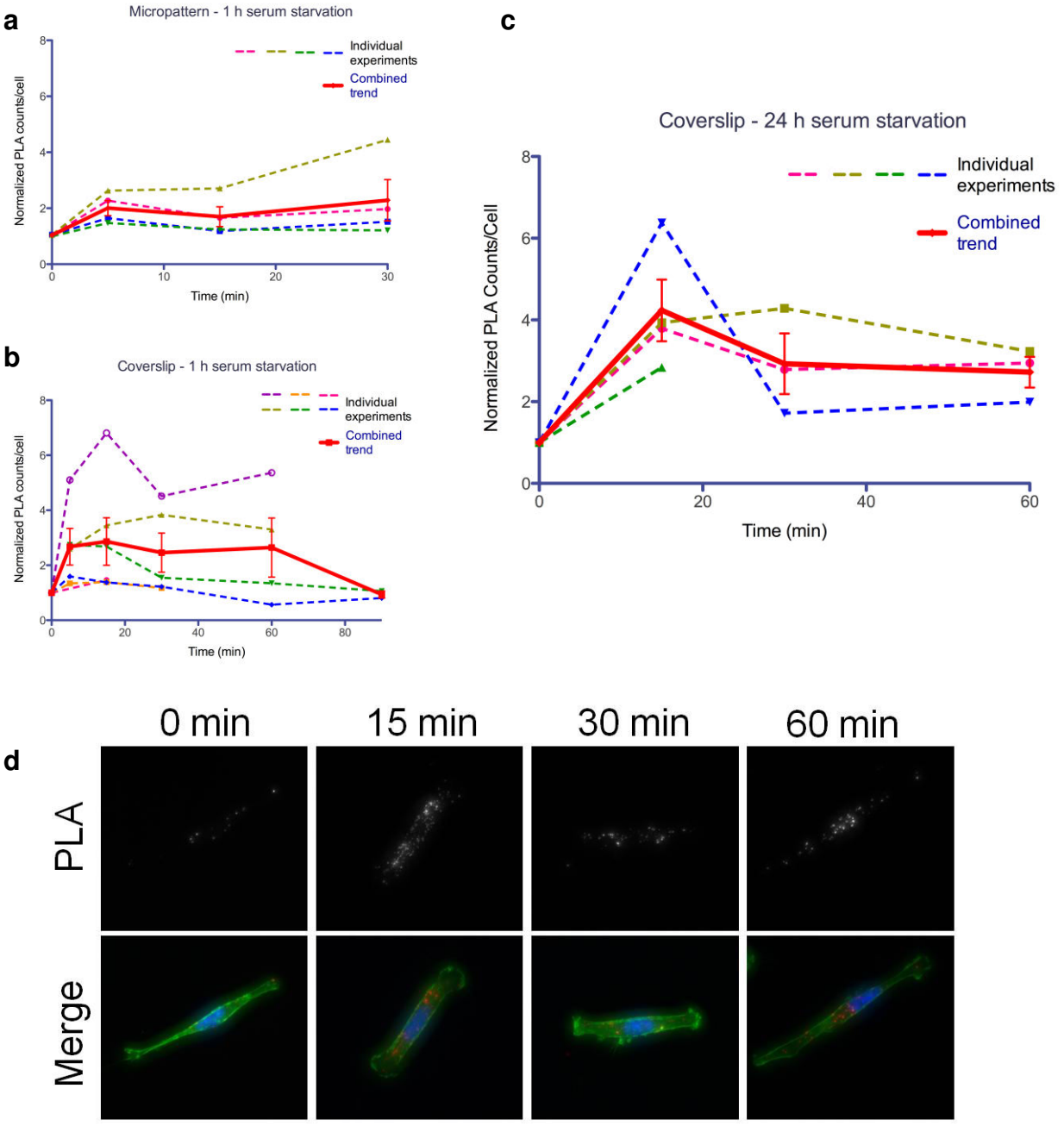

Figure 7: Quantification of the PLA signal of activated EphA2 receptors in MDA-MB-231 cells. **(a)** Cells were seeded on a micropattern and serum starved for 1 h; Stimulation with 0.5 µg/ml IgG-clustered ephrin-A5; *n* = 4 experiments **(b)** Cells were seeded on a coverslip and serum starved for 1 h; Stimulation with 0.5 µg/ml IgG-clustered ephrin-A5; *n* = 5 experiments except for 15 min, 60 min and 90 min, where *n* = 6, 4 and 2 experiments, respectively **(c)** Cells were seeded on a coverslip and serum starved for 24 h; Stimulation with 1 µg/ml IgG-clustered ephrin-A5; *n* = 3 experiments except for 15 min, where *n* = 4 experiments; Normalized PLA counts/cell are depicted; Individual experiments are shown as dotted lines, the combined trend as a continuous line; Error bars, s.e.m.; For each time point in each individual experiment an average of 10-20 cells were imaged **(d)** Representative images of the PLA signal after 24 h serum starvation and treatment with 1 µg/ml IgG-clustered ephrin-A5 in MDA-MB-231 cells; Maximum intensity Z-projection; PLA channel and composite image are depicted

Coverslip - 1h serum starvation			
Time (min)	**Mean**	**SEM**	**N**
0	1.00	0.00	6
5	2.68	0.67	5
15	2.86	0.86	6
30	2.46	0.71	5
60	2.64	1.07	4
90	0.93	0.13	2

Micropattern - 1h serum starvation			
Time (min)	**Mean**	**SEM**	**N**
0	1.00	0.00	4
5	2.00	0.27	4
15	1.70	0.35	4
30	2.29	0.73	4

Coverslip - 24h serum starvation			
Time (min)	**Mean**	**SEM**	**N**
0	1.00	0.00	4
15	4.23	0.75	4
30	2.92	0.74	3
60	2.72	0.38	3

Table 1: Mean, SEM and N values depicted for the corresponding PLA experiments with IgG-clustered ephrin-A5 shown in Fig 7.

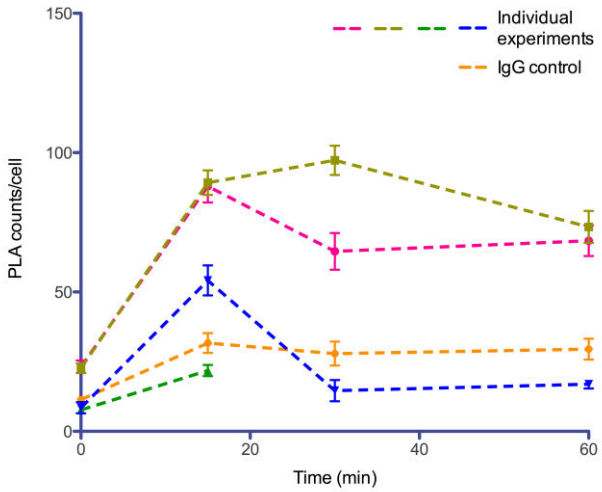

Figure 8: Quantification of the PLA signal of activated EphA2 receptors in MDA-MB-231 cells after stimulation with 1 µg/ml IgG-clustered ephrin-A5 (Individual) or 10 µg/ml IgG (IgG control) at the assigned time point (0 min, 15 min, 30 min and 60 min); PLA counts/cell are depicted; Individual experiments with treatment are shown as dotted lines; IgG control experiment is shown separately also in a dotted line; Error bars, s.e.m.; For experiments with stimulation of 1 µg/ml IgG-clustered ephrin-A5 *n* = 3 experiments except for 15 min, where *n* = 4 experiments ; For control experiment with 10 µg/ml IgG *n* = 1 experiment

Serum starvation for 24 h and plating on coverslips with stimulation of 1 µg/ml IgG-clusterd ephrin-A5 gave the highest phosphorylation of the EphA2 receptor in the systems we tested. Therefore, these conditions are also more likely to give intracellular responses after treatment with IgG-clustered ephrin-A5. Hence, these conditions were used for the subsequent optimisation experiments investigating the HRas-Erk pathway.

4.2. Elevated levels of Erk and pErk after stimulation with IgG-clustered ephrin-A5

One pathway that is known to be involved in EphA2-mediated signalling is the MAPK pathway (Fig. 2b; Fig. 4). Therefore, we aimed to show activation of the key players within the MAPK pathway in our system. As a target, Erk was chosen and its phosphorylated status was used as readout of the pathway's activation. In addition, the system was also tested without coating the coverslips with fibronectin to exclude possible side-effects originating from the fibronectin. Although we could observe an increase in the CTCF of the total cell for both Erk and pErk (Fig. 9a-d; Table 2) after stimulation with IgG-clustered ephrin-A5, the ratio pErk/Erk did not change during treatment (Fig. 9e,f; Table 2). The pErk and Erk CTCF increased 1.4-1.7 fold when the coverslips were coated with fibronectin and 1.3-1.4 fold when they were not coated (Fig. 9a-d, Table 2). Additionally, we could not observe any re-localisation of pErk to the nucleus, which is also used to show activation of Erk (Fig. 9g,h; Table 2).

Despite the fact that there is no observable increase in the fraction of pErk/Erk and no re-localisation of pErk to the nucleus observable after stimulation with 1 µg/ml IgG-clustered ephrin-A5, pErk and Erk seem to form clusters at 15 min, 30 min and 60 min after treatment in coverslips that were coated with and without fibronectin (Fig. 10a,b).

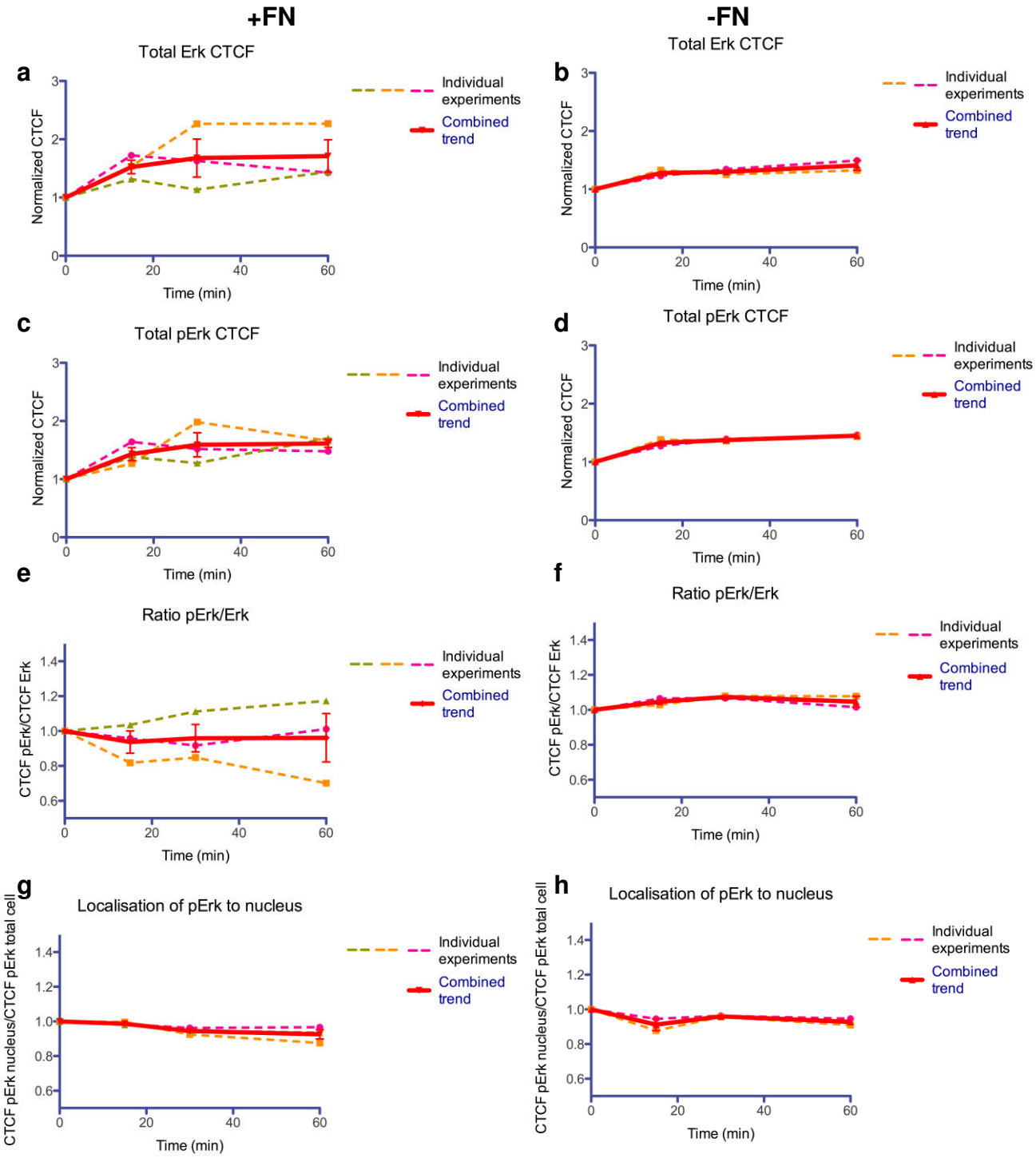

Figure 9: MDA-MB-231 cells after stimulation with 1 µg/ml IgG-clustered ephrin-A5 at the assigned time point (0 min, 15 min, 30 min and 60 min); Normalized CTCF for Erk and pErk stainings for each cell when coverslip was coated with **(a,c)** or without fibronectin **(b,d)**; Ratio of pErk/Erk in the total cell when coverslip was coated with **(e)** or without fibronectin **(f)**; Localisation of pErk to the nucleus when coverslip was coated with **(g)** or without fibronectin **(h)**; Error bars, s.e.m.; For experiments in which coverslips were coated with fibronectin $n = 3$ experiments; For experiments in which coverslips were not coated with fibronectin $n = 2$ experiments; Individual experiments are shown as dotted lines, the combined trend as a continuous line; Error bars, s.e.m.; For each time point in each individual experiment at least 20 cells were imaged

+FN	Total Erk			Total pErk		
	Mean	**SEM**	**N**	**Mean**	**SEM**	**N**
0	1.00	0.00	3	1.00	0.00	3
15	1.52	0.12	3	1.43	0.11	3
30	1.68	0.33	3	1.59	0.21	3
60	1.71	0.28	3	1.61	0.07	3

+FN	CTCF pErk/ CTCF Erk			CTCF pErk nucleus/CTCF pEkr total cell		
	Mean	**SEM**	**N**	**Mean**	**SEM**	**N**
0	1.00	0.00	3	1.00	0.00	3
15	0.94	0.06	3	0.99	0.00	3
30	0.96	0.08	3	0.95	0.01	3
60	0.96	0.14	3	0.93	0.03	3

-FN	Total Erk			Total pErk		
	Mean	**SEM**	**N**	**Mean**	**SEM**	**N**
0	1.00	0.00	2	1.00	0.00	2
15	1.28	0.05	2	1.33	0.05	2
30	1.30	0.04	2	1.38	0.02	2
60	1.41	0.08	2	1.45	0.01	2

-FN	CTCF pErk/ CTCF Erk			CTCF pErk nucleus/CTCF pEkr total cell		
	Mean	**SEM**	**N**	**Mean**	**SEM**	**N**
0	1.00	0.00	2	1.00	0.00	2
15	1.05	0.02	2	0.91	0.03	2
30	1.07	0.01	2	0.96	0.00	2
60	1.05	0.03	2	0.93	0.02	2

Table 2: Mean, SEM and N values depicted for the corresponding pErk/Erk staining experiments shown in Fig. 9.

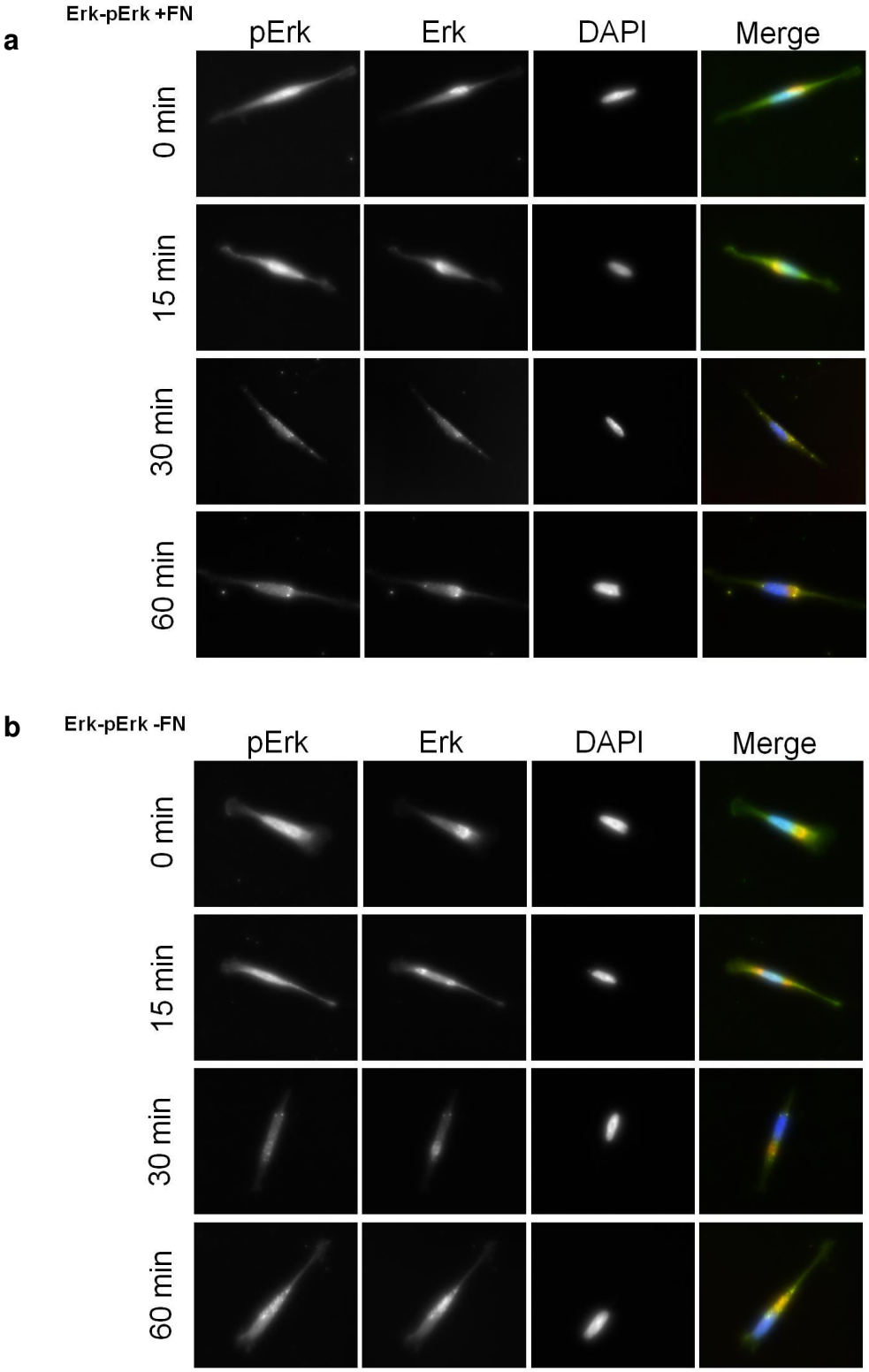

Figure 10: Representative images of the Erk and pErk stainings after 24 h serum starvation and treatment with 1 µg/ml IgG-clustered ephrin-A5 in MDA-MB-231 cells; Sum slices Z-projection; pErk channel, Erk channel, DAPI channel and composite image are depicted for each treatment time point when coverslips were coated with **(a)** or without **(b)** fibronectin

4.3. Treatment with clustered ephrin-A5 causes c-FOS activation

The MAPK pathway has multiple branches affecting different genes when stimulated by different external signals. To observe the effects on the different branches, we chose the target genes c-FOS and ELK-1. Significant up-regulation of 1.6 fold and 1.4 fold of c-Fos occurred at 30 min and 60 min, respectively, after treatment with IgG-clustered ephrin-A5 when compared to IgG treated controls (Fig. 11a; Table 3). On the contrary ELK-1 showed stable expression at the tested time points, both during stimulation and in the IgG treated controls (Fig. 11b; Table 3).

A preliminary RNA-seq experiment performed by a previous lab member uncovered that the genes CTNNA1, HK2, IRAK4 and KSR1 showed a response to treatment after IgG-clusterd ephrin-A5. As these results were obtained using a different time point after stimulation (8 h), we were investigating whether these genes also showed a response within the time frame we were performing our experiments (15 min – 90 min). Two independent RT-qPCR experiments did not show any promising changes in the expression of any of these genes (Fig. 12a; Table 4).

Despite the fact that after stimulation with IgG-clustered ephrin-A5 we could observe a significant up-regulation of c-FOS at 30 min and 60 min after treatment (Fig. 11a; Table 3), we were seeking for other target genes that might show a response to treatment. This would allow us to have a reference for the subsequent RNA-seq data. We chose to look into the genes RUNX2, FOXP1, PALLD and CCDC88A (Fig. 12b; Table 4). We could not observe any apparent changes for FOXP1 and PALLD, but changes occurred for RUNX2 and CCDC88A. Both RUNX2 and CCDC88A showed decreased expression 15 min after stimulation with 1 µg/ml IgG-clustered ephrin-A5. Levels returned to basal expression after 30 min treatment for RUNX2 and slightly increased for CCDC88A.

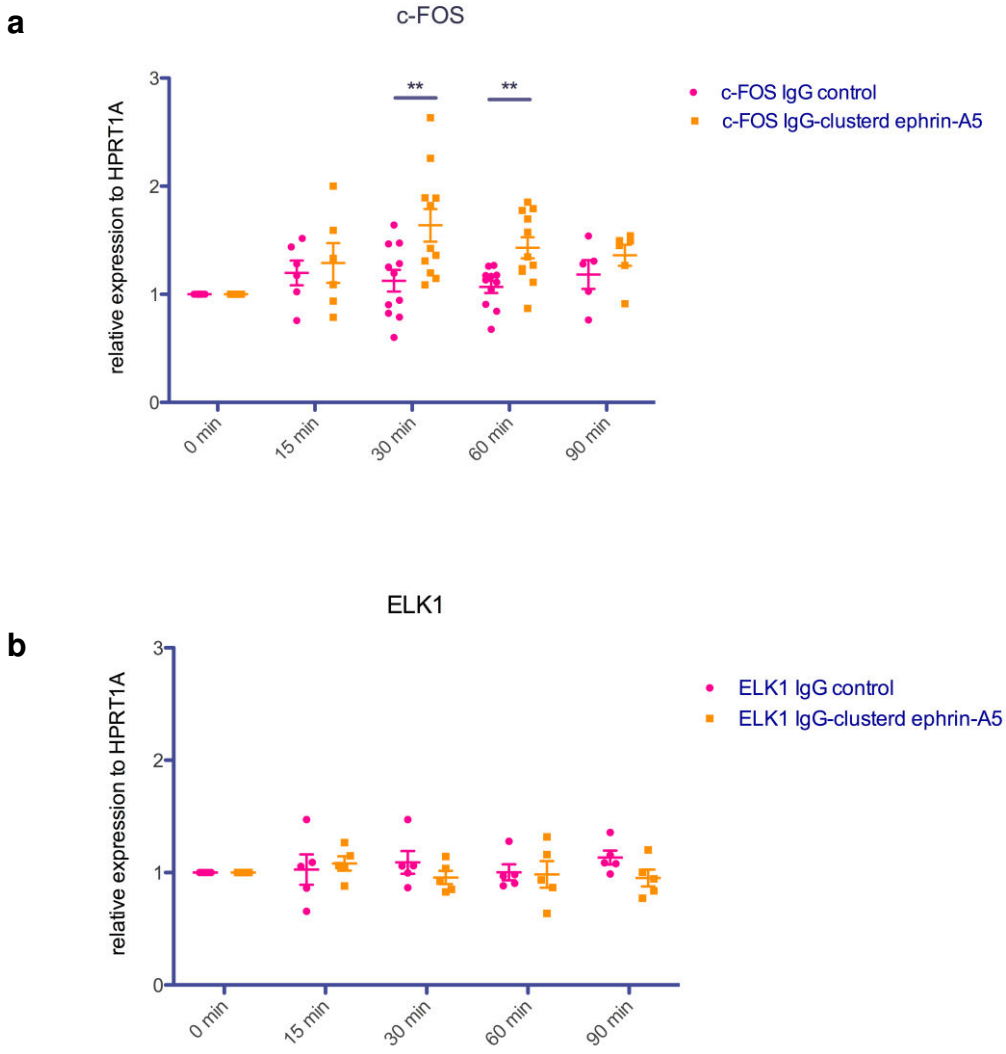

Figure 11: (a) RT-qPCR after treatment with 1 µg/ml IgG-clustered ephrin-A5 or 10 µg/ml IgG only for the target gene c-FOS; Values represent relative expression to HPRT1A; Error bars, s.e.m.; For 30 min and 60 min time points $n = 11$; For 15 min and 90 min time points $n = 6$, except for IgG treated c-FOS at 90 min, where $n = 5$ **(b)** RT-qPCR after treatment with 1 µg/ml IgG-clustered ephrin-A5 or 10 µg/ml IgG only for the target gene ELK1; Values represent relative expression to HPRT1A; Error bars, s.e.m.; $n = 5$; Wilcoxon matched-pairs signed rank test was used (** $P < 0.01$)

a

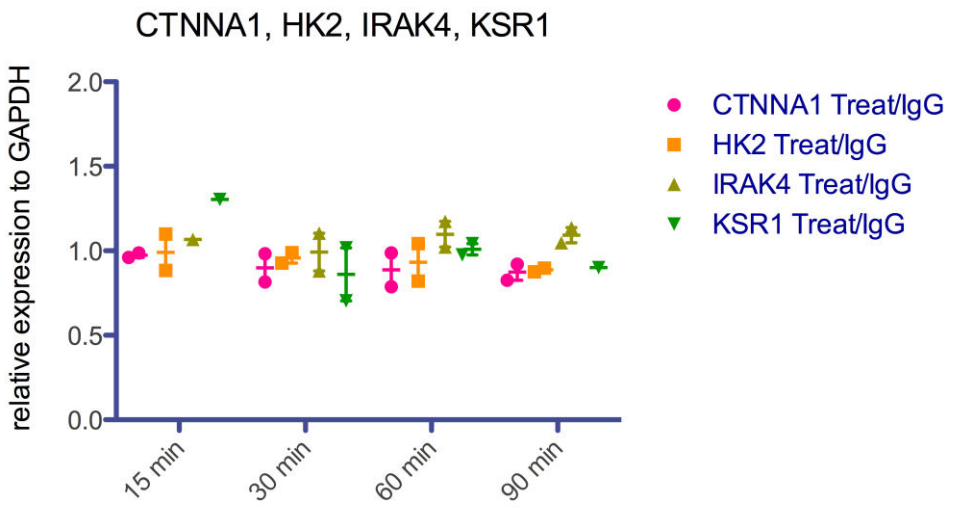

b

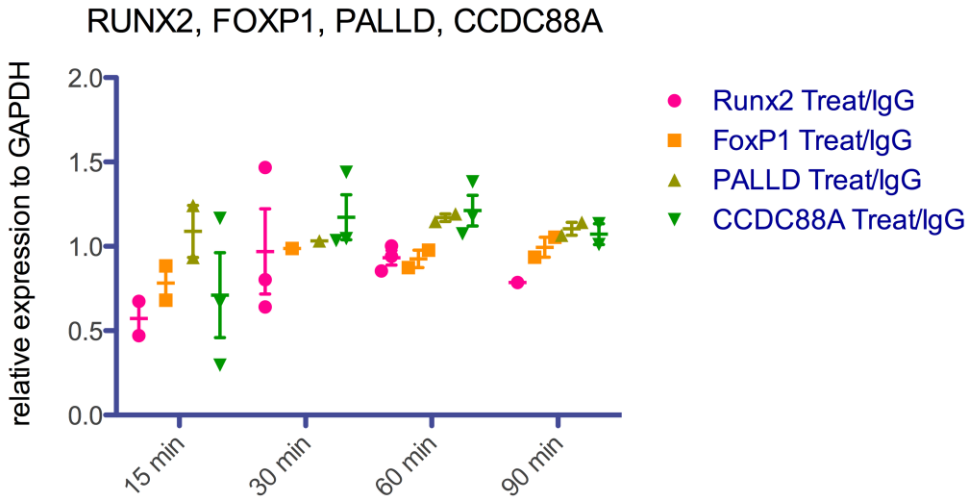

Figure 12 : RT-qPCR after treatment with 1 µg/ml IgG-clustered ephrin-A5 or 10 µg/ml IgG only for the target genes CTNNA1, HK2, IRAK4, KSR1 **(a)** and Runx2, FoxP1, PALLD, CCDC88A **(b)**; Values represent relative expression to GAPDH; Each time point was directly normalized over its corresponding IgG control treated time point; Each time point with each gene tested consists of a mixture of two independent biological replicates which were pooled equally before the RT reaction. If IgG control values were off (+/- 0.25 if compared within the IgG treated controls) values were excluded; Error bars, s.e.m.; *n* for each gene and each time point is depicted in Table 4.

	c-FOS IgG control			c-FOS IgG-clusterd ephrin-A5		
Time (min)	**Mean**	**SEM**	**N**	**Mean**	**SEM**	**N**
0	1.00	0.00	11	1.00	0.00	11
15	1.20	0.11	6	1.29	0.18	6
30	1.12	0.10	11	1.64	0.15	11
60	1.07	0.05	11	1.43	0.10	11
90	1.18	0.13	5	1.36	0.10	6

	ELK1 IgG control			ELK1 IgG-clusterd ephrin-A5		
Time (min)	**Mean**	**SEM**	**N**	**Mean**	**SEM**	**N**
0	1.00	0.00	5	1.00	0.00	5
15	1.03	0.14	5	1.08	0.06	5
30	1.09	0.10	5	0.96	0.06	5
60	1.00	0.07	5	0.98	0.12	5
90	1.13	0.06	5	0.95	0.07	5

Table 3: Mean, SEM and N values depicted for the corresponding c-FOS and ELK-1 RT-qPCR experiments shown in Fig. 11.

	CTNNA1 Treat/IgG			HK2 Treat/IgG		
Time (min)	**Mean**	**SEM**	**N**	**Mean**	**SEM**	**N**
15	0.97	0.01	2	0.99	0.11	2
30	0.90	0.08	2	0.96	0.03	2
60	0.89	0.10	2	0.93	0.11	2
90	0.87	0.05	2	0.87	0.01	2

	IRAK4 Treat/IgG			KSR1 Treat/IgG		
Time (min)	**Mean**	**SEM**	**N**	**Mean**	**SEM**	**N**
15	1.07	0.00	1	1.30	0.00	1
30	0.99	0.11	2	0.86	0.16	2
60	1.10	0.08	2	1.00	0.03	2
90	1.09	0.04	2	0.90	0.00	1

	Runx2 Treat/IgG			FoxP1 Treat/IgG		
Time (min)	**Mean**	**SEM**	**N**	**Mean**	**SEM**	**N**
15	0.57	0.10	2	0.78	0.10	2
30	0.97	0.25	3	0.99	0.00	1
60	0.93	0.04	3	0.93	0.05	2
90	0.78	0.00	1	0.99	0.06	2

	PALLD Treat/IgG			CCDC88A Treat/IgG		
Time (min)	**Mean**	**SEM**	**N**	**Mean**	**SEM**	**N**
15	1.09	0.15	2	0.71	0.25	3
30	1.03	0.00	1	1.17	0.13	3
60	1.17	0.02	2	1.21	0.09	3
90	1.10	0.04	2	1.07	0.06	2

Table 4: Mean, SEM and N values depicted for the corresponding RT-qPCR experiments shown in Fig. 12.

4.4. RT-qPCR results on RNA from individual experiments show similar trend compared to RT-qPCR results from equally pooled RNA of these individual experiments

We tested whether RT-qPCR on mRNA that was pooled equally from individual experiments after stimulation with IgG-clustered ephrin-A5 gives a similar result compared to RT-qPCR performed on the individual experiments separately. 6 individual experiments were performed and RNA was isolated as outlined previously. Prior to the reverse transcription reaction, 2 pooled samples were created, each consisting of RNA of 3 individual experiments in equal amounts. Experiments did not show a significant difference when RT-qPCR was carried out on samples with pooled or individual RNA (Fig. 13a,b; Table 5).

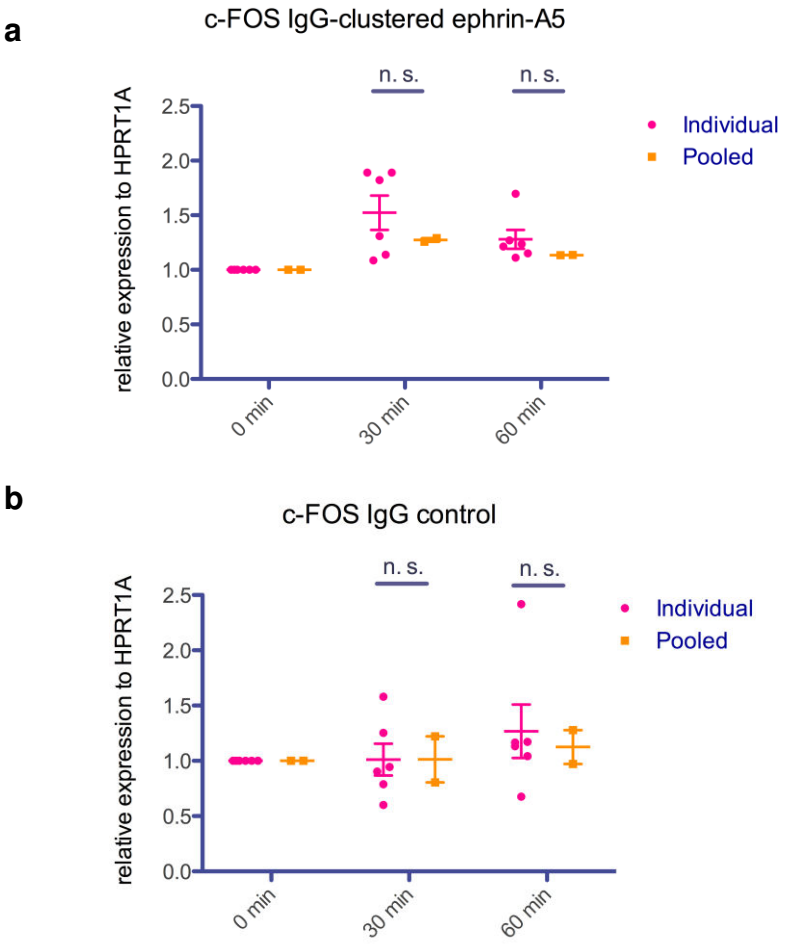

Figure 13: RT-qPCR after treatment with 1 µg/ml IgG-clustered ephrin-A5 **(a)** or 10 µg/ml IgG only **(b)** for the target gene c-FOS; Values represent relative expression to HPRT1A; Error bars, s.e.m.; For individual experiments min *n* = 6 experiments; For pooled experiments *n* = 2 experiments; Unpaired t-test was used

	c-FOS IgG control - Individual			c-FOS IgG control - Pooled		
	Mean	**SEM**	**N**	**Mean**	**SEM**	**N**
0	1.00	0.00	6	1.00	0.00	2
30	1.01	0.14	6	1.01	0.21	2
60	1.27	0.24	6	1.13	0.15	2

	c-FOS IgG-clusterd ephrin-A5 - Individual			c-FOS IgG-clusterd ephrin-A5 - Pooled		
	Mean	**SEM**	**N**	**Mean**	**SEM**	**N**
0	1.00	0.00	6	1.00	0.00	2
30	1.52	0.16	6	1.27	0.02	2
60	1.28	0.09	6	1.14	0.00	2

Table 5: Mean, SEM and N values depicted for the corresponding c-FOS experiments shown in Fig. 13.

4.5. Ephrin-A5 nanocalipers mediate tyrosine-phosphorylation of the EphA2 receptor

EphA2 receptor activation was assessed using nanocalipers that bear ephrin-A5 ligands spaced 0 nm, 40 nm and 100 nm apart (NC0, NC40, NC100). As stimulation in these experiments was performed with cells plated on coverslips, but different than previously done, we also carried out a control with IgG-clustered ephrin-A5 in parallel as a comparison between the results. A need to perform treatment differently was created as the volume for the stimulation had to be reduced due to restrictions in the amount of nanocalipers that can be produced. The exact changes that were applied are outlined above. Respective controls for each time point with either IgG or empty nanocalipers (NCempty) were carried out (Fig. 14a; Fig. 15a,b; Table 6). With a fold change of 3.5 at 15 min and 2.7 at 30 min, NC40 showed the ability to cause phosphorylation of EphA2 to almost the same extent as IgG-clustered ephrin-A5. NC100 could still promote activation of the Eph with a peak of 2.1 fold at 15 min. The lowest ability to cause phosphorylation of EphA2 showed NC0 with a fold change of 1.4 at 15 min. Overall, the controls with IgG alone and NCempty did not show activation of the EphA2 receptor, only at the 15 min time point there was a minor fold change of 1.4 for NCempty observable. The IgG-clustered ephrin-A5 control treated condition showed with a peak of activation of 4 fold at 15 min a similar and comparable extend of activation than in the previous experiments reported (Fig. 7c).

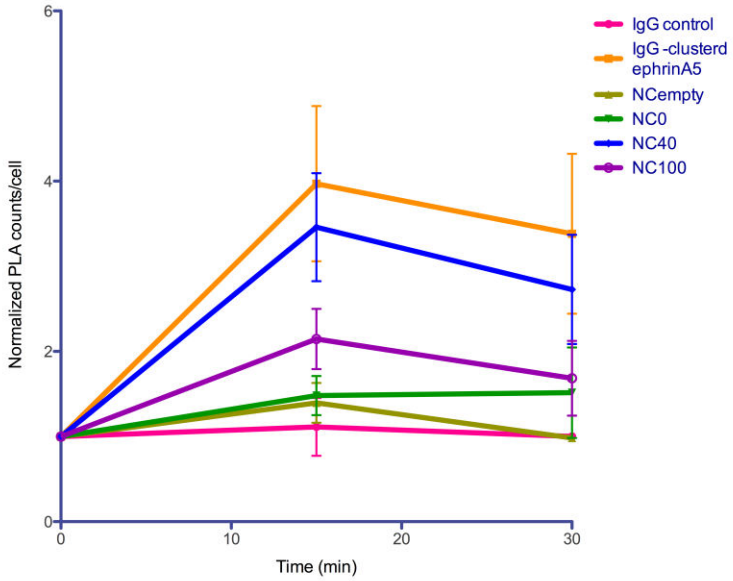

Figure 14: Quantification of the PLA signal of activated EphA2 receptors in MDA-MB-231 cells; *n* = 3 experiments except for IgG control, NCempty and NC0, where *n* = 2 experiments; Normalized PLA counts/cell are depicted; Error bars, s.e.m.; For each time point in each condition 20 cells were imaged

	IgG control			IgG-clustered ephrin A5		
Time (min)	**Mean**	**SEM**	**N**	**Mean**	**SEM**	**N**
0	1.00	0.00	2	1.00	0.00	3
15	1.11	0.34	2	3.97	0.91	3
30	1.00	0.00	2	3.38	0.94	3

	NCempty			NC0		
Time (min)	**Mean**	**SEM**	**N**	**Mean**	**SEM**	**N**
0	1.00	0.00	2	1.00	0.00	2
15	1.40	0.23	2	1.48	0.23	2
30	0.98	0.02	2	1.51	0.53	2

	NC40			NC100		
Time (min)	**Mean**	**SEM**	**N**	**Mean**	**SEM**	**N**
0	1.00	0.00	3	1.00	0.00	3
15	3.46	0.63	3	2.15	0.35	3
30	2.73	0.64	3	1.69	0.44	3

Table 6: Mean, SEM and N values depicted for the corresponding PLA experiments with IgG-clustered ephrin-A5 or nanocalipers bearing ephrin-A5 at varying distances shown in Fig. 14 and Fig. 15a,b.

a

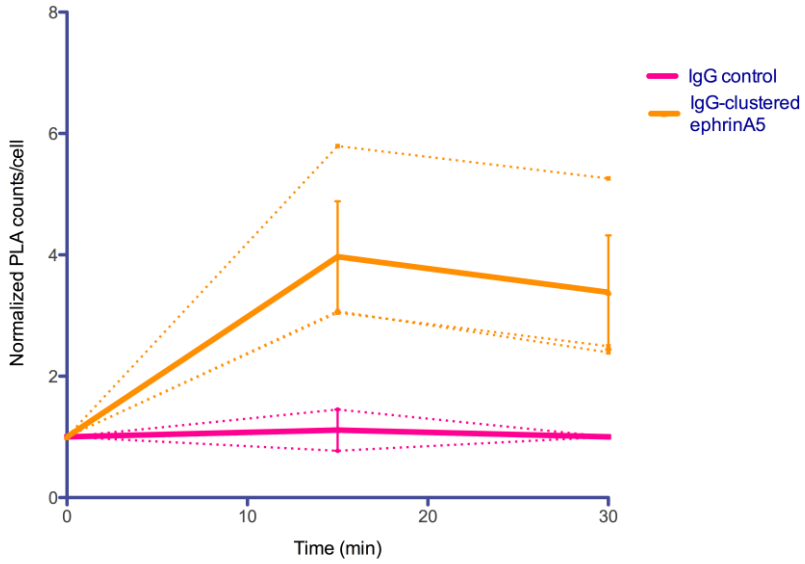

b

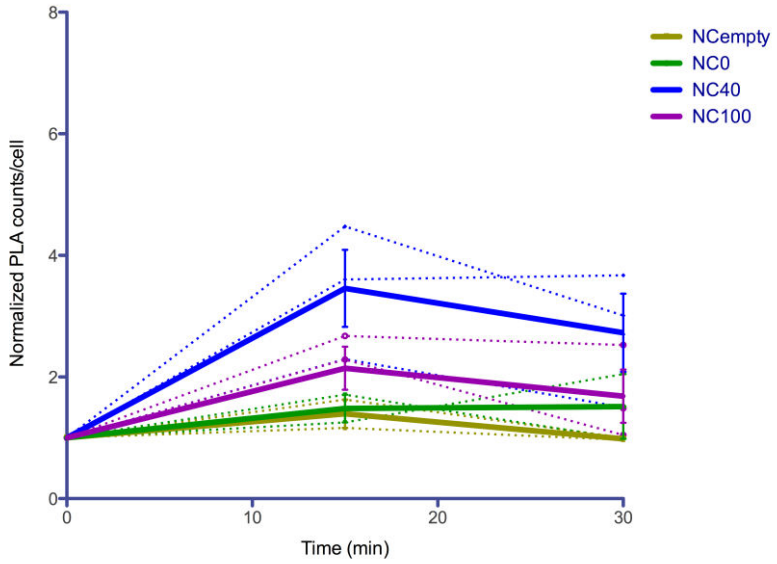

Figure 15: Alternative representation of data shown in Fig. 14; Quantification of the PLA signal of activated EphA2 receptors in MDA-MB-231 cells. **(a)** Cells were treated with IgG-clustered ephrin-A5 **(b)** Cells were treated with NC0, NC40, NC100 or NCempty; Individual experiments are represented as dotted lines, combined trend as continuous line; *n* = 3 experiments except for IgG control, NCempty and NC0, where *n* = 2 experiments; Normalized PLA counts/cell are depicted; Error bars, s.e.m.; each time point in each condition 20 cells were imaged

5. Discussion

5.1. Improvement in the extent of EphA2 receptor tyrosine-phosphorylation

The observed 4.2-fold activation of the EphA2 receptor at the 15 min time point (Fig. 7c) in our optimised system constitutes a major improvement compared to the previous attempts to activate this receptor, where the fold-change was only 1.8 fold (Shaw et. al, 2014). Changes that lead to this effect were plating the cells on coverslips coated with fibronectin instead of plating cells on micropatterns, serum starvation for 24 hours instead of 1 hour and increasing the concentration of IgG-clustered ephrin-A5 used for stimulation from 0.5 µg/ml to 1 µg/ml. Hence, using our system it is more likely to observe intracellular effects caused by EphA2 after stimulation with ephrin-A5 ligands. However, the actual fraction of tyrosine phosphorylated EphA2 receptors over the total EphA2 receptors present on the cell might be higher at later time points, as binding of ligands leads to internalisation of EphA2 and removal from the cell surface (Binda et al., 2012).

5.2. Clustering of Erk is induced after treatment with IgG-clustered ephrin-A5

Fibronectin coating did not affect the elevation of the Erk and pErk levels (Fig. 9a-d). In addition, there was no apparent difference in the pErk/Erk ratios (Fig. 9e,f) and in the localisation to the nucleus (Fig. 9g,h) if the coverslips were coated with or without fibronectin. Nevertheless, the results suggest that if the coverslips are not coated with fibronectin, the HRas-Erk pathway seems to be more stable than using the coverslips without coating. This might be due to the fact that coating with fibronectin leads to activation of the MAPK pathway (Zhang et al., 2002), among many other pathways. Furthermore, the microscope images suggest that in both cases already in the 0 min time point a substantial amount of Erk and pErk is localised at the nucleus (Fig. 10a,b) due to a mutation in B-Raf and an activated allele of KRAS in MDA-MB-231 cells (Wilhelm et al., 2004; Ogata et al., 2001; Kozma et al., 1987).

Although there was no increased fraction of pErk/Erk in the stimulated conditions (Fig. 9e,f), activation of Erk might still occur. Clustering of Erk could only be observed in cells that were exposed to treatment. Ephrin-A1 treatment triggers the formation of EphA2-associated complex involving Src and focal adhesion kinase (FAK) (Parri et al., 2007). Src in turn can bind to the scaffolding protein β-arrestin (Miller and Lefkowitz, 2001) that is known to bind to Erk (DeFea et al., 2000; Strungs and Luttrell, 2014). This might explain the observed clustering of Erk upon treatment.

Moreover, Erk plays a role in adhesion disassembly (Webb et al., 2004) and is recruited to newly forming cell-matrix adhesions (Fincham et al., 2000), associating Erk with the cytoskeletal network and cell motility (Huang et al., 2004). As Eph receptor activation is modulating the actin cytoskeleton and having an impact on intracellular adhesion molecules and thereby controls cell morphology, migration and adhesion (Pasquale, 2010), this might be another link to the observed clustering of Erk after stimulation with IgG-clustered ephrin-A5.

In addition, Sef is known to bind and localise MEK and Erk to the Golgi apparatus, thereby allowing specific activation of cytoplasmic targets of Erk but preventing translocation of Erk to the nucleus (Philips, 2004). This could represent another explanation for the observed clustering of Erk upon treatment.

5.3. Expression profiles of genes investigated serve as references for RNA-seq experiments

We found some genes differentially expressed in MDA-MB-231 cells after stimulation with IgG-clustered ephrin-A5 when compared to IgG control treated cells. These genes are c-FOS, RUNX2 and CCDC88A (Fig. 11a; Fig. 12b). Their changed expression profiles represent useful reference data for the prospective RNA-seq. Expression of c-FOS gives a reference for the time points 30 min and 60 min after stimulation with IgG-clustered ephrin-A5, whereas RUNX2 and CCDC88A give reference data for 15 min after stimulation. However, experiments with RUNX2 and

CCDC88A need to be repeated to show that changes at the 15 min time point are stable. Obtained expression profiles of the genes ELK1, CTNNA1, HK2, IRAK4, KSR1, PALLD and FOXP1 did not show any apparent changes during stimulation with IgG-clustered ephrin A5 (Fig. 11b; Fig. 12a). They also represent reference data for the RNA-seq since no changes in their expression should occur during treatment throughout the time points tested.

5.4. Reduction in RNA-seq experiments through pooling of RNA

As already outlined, the final goal of this project is to perform RNA-seq and evaluate the initial response of MDA-MB-231 cells to treatment with nanocalipers that bear ephrin-A5 ligands that are differentially spaced apart. Obtaining the RT-qPCR data of the known target genes, we realised that MDA-MB-231 cells are rather unstable in their expression. We could show that RT-qPCR results for which starting RNA originated from a pool of 3 individual experiments are similar and give less variation compared to the RT-qPCR results for the individual experiments alone (Fig. 13; Table 5). This reduces the number of runs that are necessary for the final RNA-seq experiments as biological variance between different samples can already be reduced in the pooled RNA of individual experiments.

5.5. NC40 shows higher potential to cause EphA2 tyrosine-phosphorylation than NC0 and NC100

As reported previously, NC40 elicits a higher response upon stimulation than both NC0 and NC100 and that this response is close to the extent of EphA2 receptor phosphorylation promoted when treatment with IgG-clustered ephrin-A5 occurs (Fig. 14; Fig. 15a,b) (Shaw et. al, 2014). NC0 stimulation might only represent background, as the 15 min control NCempty treatment also gives the same response (Table 6).

5.6. Future perspectives

The next steps in this project involve testing of target genes by RT-qPCR when MDA-MB-231 cells are treated with ephrin-A5 nanocalipers. Finally, RNA-seq will be performed by pooling RNA of several experiments and the initial response on the transcriptome will be evaluated at different time points. This will shed light on the underlying mechanism of the inhibitory effects of differentially nano-spatially distributed ephrin-A5 ligands on invasive MDA-MB-231 breast cancer cells.

6. Acknowledgments

I want to acknowledge several people who provided support throughout my time here at the Karolinska Institutet, Sweden. Foremost, I want to mention Ana Teixeira for hosting my internship and giving me the opportunity to be at this institute. Furthermore, I am very thankful for all the support with my thesis, help and advice Toon Verheyen provided me and for the tremendous amount of time he spent on teaching me how to work scientifically. In addition, I want to thank Alan Shaw and Björn Högberg to provide me with the nanocalipers for the respective experiments. I also want to thank Friedrich Propst for supervising my thesis. I also want to thank the Erasmus + programme for supporting me financially during my stay.

Particularly, I want to thank my whole family and friends for encouraging and helping me in every possible way and enabling me to pursue my studies and this internship.

7. References

Abraham, S., Knapp, D.W., Cheng, L., Snyder, P.W., Mittal, S.K., Bangari, D.S., Kinch, M., Wu, L., Dhariwal, J., and Mohammed, S.I. (2006). Expression of EphA2 and Ephrin A-1 in carcinoma of the urinary bladder. Clin. Cancer Res. 12, 353–360.

Alford, S., Watson-Hurthig, A., Scott, N., Carette, A., Lorimer, H., Bazowski, J., and Howard, P.L. (2010). Soluble ephrin a1 is necessary for the growth of HeLa and SK-BR3 cells. Cancer Cell Int. 10, 41.

Beauchamp, A., and Debinski, W. (2012). Ephs and ephrins in cancer: ephrin-A1 signalling. Semin. Cell Dev. Biol. 23, 109–115.

Benson, E., Mohammed, A., Gardell, J., Masich, S., Czeizler, E., Orponen, P., and Högberg, B. (2015). DNA rendering of polyhedral meshes at the nanoscale. Nature 523, 441–444.

Binda, E., Visioli, A., Giani, F., Lamorte, G., Copetti, M., Pitter, K.L., Huse, J.T., Cajola, L., Zanetti, N., DiMeco, F., et al. (2012). The EphA2 receptor drives self-renewal and tumorigenicity in stem-like tumor-propagating cells from human glioblastomas. Cancer Cell 22, 765–780.

Björn Högberg (n.d.). Retrieved from http://www.hogberglab.net/

Boyd, A.W., Bartlett, P.F., and Lackmann, M. (2014). Therapeutic targeting of EPH receptors and their ligands. Nat Rev Drug Discov 13, 39–62.

Buricchi, F., Giannoni, E., Grimaldi, G., Parri, M., Raugei, G., Ramponi, G., and Chiarugi, P. (2007). Redox regulation of ephrin/integrin cross-talk. Cell Adhesion & Migration 1, 33–42.

Cheng, N., Brantley, D.M., Liu, H., Lin, Q., Enriquez, M., Gale, N., Yancopoulos, G., Cerretti, D.P., Daniel, T.O., and Chen, J. (2002). Blockade of EphA receptor tyrosine kinase activation inhibits vascular endothelial cell growth factor-induced angiogenesis. Mol. Cancer Res. 1, 2–11.

Chin, Y.R., and Toker, A. (2010). The actin-bundling protein palladin is an Akt1-specific substrate that regulates breast cancer cell migration. Mol. Cell 38, 333–344.

Cui, X.-D., Lee, M.-J., Yu, G.-R., Kim, I.-H., Yu, H.-C., Song, E.-Y., and Kim, D.-G. (2010). EFNA1 ligand and its receptor EphA2: potential biomarkers for hepatocellular carcinoma. Int. J. Cancer 126, 940–949.

Davis, S., Gale, N.W., Aldrich, T.H., Maisonpierre, P.C., Lhotak, V., Pawson, T., Goldfarb, M., and Yancopoulos, G.D. (1994). Ligands for EPH-related receptor tyrosine kinases that require membrane attachment or clustering for activity. Science 266, 816–819.

DeFea, K.A., Vaughn, Z.D., O'Bryan, E.M., Nishijima, D., Déry, O., and Bunnett, N.W. (2000). The proliferative and antiapoptotic effects of substance P are facilitated by formation of a beta -arrestin-dependent scaffolding complex. Proc. Natl. Acad. Sci. U.S.A. 97, 11086–11091.

Easty, D.J., Guthrie, B.A., Maung, K., Farr, C.J., Lindberg, R.A., Toso, R.J., Herlyn, M., and Bennett, D.C. (1995). Protein B61 as a new growth factor: expression of B61 and up-regulation of its receptor epithelial cell kinase during melanoma progression. Cancer Res. 55, 2528–2532.

Enomoto, A., Ping, J., and Takahashi, M. (2006). Girdin, a novel actin-binding protein, and its family of proteins possess versatile functions in the Akt and Wnt signaling pathways. Ann. N. Y. Acad. Sci. 1086, 169–184.

Fang, W.B., Brantley-Sieders, D.M., Hwang, Y., Ham, A.-J.L., and Chen, J. (2008a). Identification and Functional Analysis of Phosphorylated Tyrosine Residues within EphA2 Receptor Tyrosine Kinase. J Biol Chem 283, 16017–16026.

Fang, W.B., Ireton, R.C., Zhuang, G., Takahashi, T., Reynolds, A., and Chen, J. (2008b). Overexpression of EPHA2 receptor destabilizes adherens junctions via a RhoA-dependent mechanism. J. Cell. Sci. 121, 358–368.

Fincham, V.J., James, M., Frame, M.C., and Winder, S.J. (2000). Active ERK/MAP kinase is targeted to newly forming cell-matrix adhesions by integrin engagement and v-Src. EMBO J. 19, 2911–2923.

Fox, B.P., and Kandpal, R.P. (2004). Invasiveness of breast carcinoma cells and transcript profile: Eph receptors and ephrin ligands as molecular markers of potential diagnostic and prognostic application. Biochem. Biophys. Res. Commun. 318, 882–892.

Georgakopoulos, A., Litterst, C., Ghersi, E., Baki, L., Xu, C., Serban, G., and Robakis, N.K. (2006). Metalloproteinase/Presenilin1 processing of ephrinB regulates EphB-induced Src phosphorylation and signalling. EMBO J. 25, 1242–1252.

Greene, A.C., Lord, S.J., Tian, A., Rhodes, C., Kai, H., and Groves, J.T. (2014). Spatial Organization of EphA2 at the Cell-Cell Interface Modulates Trans-Endocytosis of EphrinA1. Biophys J 106, 2196–2205.

Gu, C., and Park, S. (2001). The EphA8 receptor regulates integrin activity through p110gamma phosphatidylinositol-3 kinase in a tyrosine kinase activity-independent manner. Mol. Cell. Biol. 21, 4579–4597.

Halacli, S.O., and Dogan, A.L. (2015). FOXP1 regulation via the PI3K/Akt/p70S6K signaling pathway in breast cancer cells. Oncol Lett 9, 1482–1488.

Hattori, M., Osterfield, M., and Flanagan, J.G. (2000). Regulated cleavage of a contact-mediated axon repellent. Science 289, 1360–1365.

Himanen, J.-P., Saha, N., and Nikolov, D.B. (2007). Cell-cell signalling via Eph receptors and ephrins. Curr. Opin. Cell Biol. 19, 534–542.

Holm, R., de Putte, G.V., Suo, Z., Lie, A.K., and Kristensen, G.B. (2008). Expressions of EphA2 and EphrinA-1 in early squamous cell cervical carcinomas and their relation to prognosis. Int J Med Sci 5, 121–126.

Huang, C., Jacobson, K., and Schaller, M.D. (2004). MAP kinases and cell migration. J Cell Sci 117, 4619–4628.

Iwasato, T., Katoh, H., Nishimaru, H., Ishikawa, Y., Inoue, H., Saito, Y.M., Ando, R., Iwama, M., Takahashi, R., Negishi, M., et al. (2007). Rac-GAP alpha-chimerin regulates motor-circuit formation as a key mediator of EphrinB3/EphA4 forward signalling. Cell 130, 742–753.

Jørgensen, C., Sherman, A., Chen, G.I., Pasculescu, A., Poliakov, A., Hsiung, M., Larsen, B., Wilkinson, D.G., Linding, R., and Pawson, T. (2009). Cell-specific information processing in segregating populations of Eph receptor ephrin-expressing cells. Science 326, 1502–1509.

Kikawa, K.D., Vidale, D.R., Van Etten, R.L., and Kinch, M.S. (2002). Regulation of the EphA2 kinase by the low molecular weight tyrosine phosphatase induces transformation. J. Biol. Chem. 277, 39274–39279.

Kozma, S.C., Bogaard, M.E., Buser, K., Saurer, S.M., Bos, J.L., Groner, B., and Hynes, N.E. (1987). The human c-Kirsten ras gene is activated by a novel mutation in codon 13 in the breast carcinoma cell line MDA-MB231. Nucleic Acids Res 15, 5963–5971.

Lin, K.-T., Sloniowski, S., Ethell, D.W., and Ethell, I.M. (2008). Ephrin-B2-induced cleavage of EphB2 receptor is mediated by matrix metalloproteinases to trigger cell repulsion. J. Biol. Chem. 283, 28969–28979.

Litterst, C., Georgakopoulos, A., Shioi, J., Ghersi, E., Wisniewski, T., Wang, R., Ludwig, A., and Robakis, N.K. (2007). Ligand binding and calcium influx induce distinct ectodomain/gamma-secretase-processing pathways of EphB2 receptor. J. Biol. Chem. 282, 16155–16163.

Macrae, M., Neve, R.M., Rodriguez-Viciana, P., Haqq, C., Yeh, J., Chen, C., Gray, J.W., and McCormick, F. (2005). A conditional feedback loop regulates Ras activity through EphA2. Cancer Cell 8, 111–118.

Matsuoka, H., Obama, H., Kelly, M.L., Matsui, T., and Nakamoto, M. (2005). Biphasic functions of the kinase-defective Ephb6 receptor in cell adhesion and migration. J. Biol. Chem. 280, 29355–29363.

Miao, H., Burnett, E., Kinch, M., Simon, E., and Wang, B. (2000). Activation of EphA2 kinase suppresses integrin function and causes focal-adhesion-kinase dephosphorylation. Nature Cell Biology 2, 62–69.

Miao, H., Wei, B.R., Peehl, D.M., Li, Q., Alexandrou, T., Schelling, J.R., Rhim, J.S., Sedor, J.R., Burnett, E., and Wang, B. (2001). Activation of EphA receptor tyrosine kinase inhibits the Ras/MAPK pathway. Nat. Cell Biol. 3, 527–530.

Miao, H., Li, D.-Q., Mukherjee, A., Guo, H., Petty, A., Cutter, J., Basilion, J.P., Sedor, J., Wu, J., Danielpour, D., et al. (2009). EphA2 mediates ligand-dependent inhibition and ligand-independent promotion of cell migration and invasion via a reciprocal regulatory loop with Akt. Cancer Cell 16, 9–20.

Miller, W.E., and Lefkowitz, R.J. (2001). Expanding roles for β-arrestins as scaffolds and adapters in GPCR signalling and trafficking. Current Opinion in Cell Biology 13, 139–145.

Miura, K., Nam, J.-M., Kojima, C., Mochizuki, N., and Sabe, H. (2009). EphA2 engages Git1 to suppress Arf6 activity modulating epithelial cell-cell contacts. Mol. Biol. Cell 20, 1949–1959.

Nie, D., Di Nardo, A., Han, J.M., Baharanyi, H., Kramvis, I., Huynh, T., Dabora, S., Codeluppi, S., Pandolfi, P.P., Pasquale, E.B., et al. (2010). Tsc2-Rheb signalling regulates EphA-mediated axon guidance. Nat. Neurosci. 13, 163–172.

Nievergall, E., Janes, P.W., Stegmayer, C., Vail, M.E., Haj, F.G., Teng, S.W., Neel, B.G., Bastiaens, P.I., and Lackmann, M. (2010). PTP1B regulates Eph receptor function and trafficking. J. Cell Biol. 191, 1189–1203.

Nikolov, D.B., Xu, K., and Himanen, J.P. (2013). Eph/ephrin recognition and the role of Eph/ephrin clusters in signalling initiation. Biochim. Biophys. Acta 1834, 2160–2165.

Noberini, R., Lamberto, I., and Pasquale, E.B. (2012). Targeting Eph Receptors with Peptides and Small Molecules: Progress and Challenges. Semin Cell Dev Biol 23, 51–57.

Noren, N.K., and Pasquale, E.B. (2004). Eph receptor-ephrin bidirectional signals that target Ras and Rho proteins. Cell. Signal. 16, 655–666.

Ogata, H., Sato, H., Takatsuka, J., and De Luca, L.M. (2001). Human breast cancer MDA-MB-231 cells fail to express the neurofibromin protein, lack its type I mRNA isoform and show accumulation of P-MAPK and activated Ras. Cancer Letters 172, 159–164.

Orsulic, S., and Kemler, R. (2000). Expression of Eph receptors and ephrins is differentially regulated by E-cadherin. J. Cell. Sci. 113 (Pt 10), 1793–1802.

Pandey, A., Lazar, D.F., Saltiel, A.R., and Dixit, V.M. (1994). Activation of the Eck receptor protein tyrosine kinase stimulates phosphatidylinositol 3-kinase activity. Journal of Biological Chemistry 269, 30154–30157.

Pandey, A., Shao, H., Marks, R.M., Polverini, P.J., and Dixit, V.M. (1995). Role of B61, the ligand for the Eck receptor tyrosine kinase, in TNF-alpha-induced angiogenesis. Science 268, 567–569.

Parri, M., Buricchi, F., Giannoni, E., Grimaldi, G., Mello, T., Raugei, G., Ramponi, G., and Chiarugi, P. (2007). EphrinA1 Activates a Src/Focal Adhesion Kinase-mediated

Motility Response Leading to Rho-dependent Actino/Myosin Contractility. J. Biol. Chem. 282, 19619–19628.

Pasquale, E.B. (2005). Eph receptor signalling casts a wide net on cell behaviour. Nat Rev Mol Cell Biol 6, 462–475.

Pasquale, E.B. (2008). Eph-Ephrin Bidirectional Signalling in Physiology and Disease. Cell 133, 38–52.

Pasquale, E.B. (2010). Eph receptors and ephrins in cancer: bidirectional signalling and beyond. Nat Rev Cancer 10, 165–180.

Philips, M.R. (2004). Sef: A MEK/ERK Catcher on the Golgi. Molecular Cell 15, 168–169.

Pitulescu, M.E., and Adams, R.H. (2010). Eph/ephrin molecules--a hub for signalling and endocytosis. Genes Dev. 24, 2480–2492.

Pratt, R.L., and Kinch, M.S. (2002). Activation of the EphA2 tyrosine kinase stimulates the MAP/ERK kinase signalling cascade. Oncogene 21, 7690–7699.

Pratt, R.L., and Kinch, M.S. (2003). Ligand binding up-regulates EphA2 messenger RNA through the mitogen-activated protein/extracellular signal-regulated kinase pathway. Mol. Cancer Res. 1, 1070–1076.

Richter, M., Murai, K.K., Bourgin, C., Pak, D.T., and Pasquale, E.B. (2007). The EphA4 receptor regulates neuronal morphology through SPAR-mediated inactivation of Rap GTPases. J. Neurosci. 27, 14205–14215.

Shamah, S.M., Lin, M.Z., Goldberg, J.L., Estrach, S., Sahin, M., Hu, L., Bazalakova, M., Neve, R.L., Corfas, G., Debant, A., et al. (2001). EphA Receptors Regulate Growth Cone Dynamics through the Novel Guanine Nucleotide Exchange Factor Ephexin. Cell 105, 233–244.

Shaw, A., Lundin, V., Petrova, E., Fördős, F., Benson, E., Al-Amin, A., Herland, A., Blokzijl, A., Högberg, B., and Teixeira, A.I. (2014). Spatial control of membrane receptor function using ligand nanocalipers. Nat Meth 11, 841–846.

Shintani, T., Ihara, M., Sakuta, H., Takahashi, H., Watakabe, I., and Noda, M. (2006). Eph receptors are negatively controlled by protein tyrosine phosphatase receptor type O. Nat. Neurosci. 9, 761–769.

Söderberg, O., Gullberg, M., Jarvius, M., Ridderstråle, K., Leuchowius, K.-J., Jarvius, J., Wester, K., Hydbring, P., Bahram, F., Larsson, L.-G., et al. (2006). Direct observation of individual endogenous protein complexes in situ by proximity ligation. Nat Meth 3, 995–1000.

Stein, E., Cerretti, D.P., and Daniel, T.O. (1996). Ligand activation of ELK receptor tyrosine kinase promotes its association with Grb10 and Grb2 in vascular endothelial cells. J. Biol. Chem. 271, 23588–23593.

Stein, E., Lane, A.A., Cerretti, D.P., Schoecklmann, H.O., Schroff, A.D., Van Etten, R.L., and Daniel, T.O. (1998). Eph receptors discriminate specific ligand oligomers to determine alternative signalling complexes, attachment, and assembly responses. Genes Dev. 12, 667–678.

Strungs, E.G., and Luttrell, L.M. (2014). Arrestin-dependent activation of ERK and Src family kinases. Handb Exp Pharmacol 219, 225–257.

Tanaka, M., Sasaki, K., Kamata, R., and Sakai, R. (2007). The C-terminus of ephrin-B1 regulates metalloproteinase secretion and invasion of cancer cells. J. Cell. Sci. 120, 2179–2189.

Tandon, M., Chen, Z., and Pratap, J. (2014). Runx2 activates PI3K/Akt signaling via mTORC2 regulation in invasive breast cancer cells. Breast Cancer Res. 16, R16.

Thaker, P.H., Deavers, M., Celestino, J., Thornton, A., Fletcher, M.S., Landen, C.N., Kinch, M.S., Kiener, P.A., and Sood, A.K. (2004). EphA2 expression is associated with aggressive features in ovarian carcinoma. Clin. Cancer Res. 10, 5145–5150.

Webb, D.J., Donais, K., Whitmore, L.A., Thomas, S.M., Turner, C.E., Parsons, J.T., and Horwitz, A.F. (2004). FAK–Src signalling through paxillin, ERK and MLCK regulates adhesion disassembly. Nat Cell Biol 6, 154–161.

Weibrecht, I., Leuchowius, K.-J., Clausson, C.-M., Conze, T., Jarvius, M., Howell, W.M., Kamali-Moghaddam, M., and Söderberg, O. (2010). Proximity ligation assays: a recent addition to the proteomics toolbox. Expert Rev Proteomics 7, 401–409.

Wilhelm, S.M., Carter, C., Tang, L., Wilkie, D., McNabola, A., Rong, H., Chen, C., Zhang, X., Vincent, P., McHugh, M., et al. (2004). BAY 43-9006 exhibits broad spectrum oral antitumor activity and targets the RAF/MEK/ERK pathway and

receptor tyrosine kinases involved in tumor progression and angiogenesis. Cancer Res. 64, 7099–7109.

Wilkinson, D.G. (2001). Multiple roles of eph receptors and ephrins in neural development. Nat Rev Neurosci 2, 155–164.

Wykosky, J., Gibo, D.M., Stanton, C., and Debinski, W. (2005). EphA2 as a novel molecular marker and target in glioblastoma multiforme. Mol. Cancer Res. 3, 541–551.

Wykosky, J., Palma, E., Gibo, D., Ringler, S., Turner, C., and Debinski, W. (2008). Soluble monomeric EphrinA1 is released from tumor cells and is a functional ligand for the EphA2 receptor. Oncogene 27, 7260–7273.

Yamazaki, T., Masuda, J., Omori, T., Usui, R., Akiyama, H., and Maru, Y. (2009). EphA1 interacts with integrin-linked kinase and regulates cell morphology and motility. J. Cell. Sci. 122, 243–255.

Yang, N.-Y., Fernandez, C., Richter, M., Xiao, Z., Valencia, F., Tice, D.A., and Pasquale, E.B. (2011). Crosstalk of the EphA2 receptor with a serine/threonine phosphatase suppresses the Akt-mTORC1 pathway in cancer cells. Cellular Signalling 23, 201–212.

Yuan, W.-J., Ge, J., Chen, Z.-K., Wu, S.-B., Shen, H., Yang, P., Hu, B., Zhang, G.-W., and Chen, Z.-H. (2009). Over-expression of EphA2 and EphrinA-1 in human gastric adenocarcinoma and its prognostic value for postoperative patients. Dig. Dis. Sci. 54, 2410–2417.

Yumoto, N., Wakatsuki, S., Kurisaki, T., Hara, Y., Osumi, N., Frisén, J., and Sehara-Fujisawa, A. (2008). Meltrin beta/ADAM19 interacting with EphA4 in developing neural cells participates in formation of the neuromuscular junction. PLoS ONE 3, e3322.

Zantek, N.D., Azimi, M., Fedor-Chaiken, M., Wang, B., Brackenbury, R., and Kinch, M.S. (1999). E-Cadherin Regulates the Function of the EphA2 Receptor Tyrosine Kinase. Cell Growth Differ 10, 629–638.

Zelinski, D.P., Zantek, N.D., Stewart, J.C., Irizarry, A.R., and Kinch, M.S. (2001). EphA2 overexpression causes tumorigenesis of mammary epithelial cells. Cancer Res. 61, 2301–2306.

Zhang, L., Bewick, M., and Lafrenie, R.M. (2002). Role of Raf-1 and FAK in cell density-dependent regulation of integrin-dependent activation of MAP kinase. Carcinogenesis 23, 1251–1258.

Zhou, Y., Yamada, N., Tanaka, T., Hori, T., Yokoyama, S., Hayakawa, Y., Yano, S., Fukuoka, J., Koizumi, K., Saiki, I., et al. (2015). Crucial roles of RSK in cell motility by catalysing serine phosphorylation of EphA2. Nat Commun 6, 7679.

Zhuang, G., Hunter, S., Hwang, Y., and Chen, J. (2007). Regulation of EphA2 receptor endocytosis by SHIP2 lipid phosphatase via phosphatidylinositol 3-Kinase-dependent Rac1 activation. J. Biol. Chem. 282, 2683–2694.

PERSONAL INFORMATION

Dominik Lindenhofer

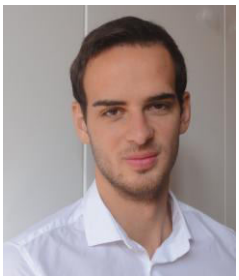

Einsiedlergasse 52 13/14
1050 Vienna, Austria
+43664 3538879

dominik.lindenhofer5@gmail.com

Date of birth 27th of June, 1991 | Nationality Austrian

WORK EXPERIENCE

January 2015 – October 2015

Internship at the Karolinska Institutet, Stockholm, SWE

Reserach Group Ana Teixeira, Research Division of Biomaterials and Regenerative Medicine, Department of Medical Biochemistry and Biophysics, Karolinska Institutet (SWE)

- Modulation of the MAPK pathway by differential nano-spatial distribution of ephrins to Eph receptors

February 2014 – May 2014
August 2014
December 2014

Center for Anatomy and Cell Biology, Vienna, AUT

Research Group Walter Rossmanith, Center for Anatomy and Cell Biology, Medical University of Vienna (AUT)

- Proteinaceous RNase P (PRORP) mediated maturation of tRNA variants
- Single turnover kinetic experiments
- Experiments with P^{32}

January 2013 – July 2013

Internship at the LICR, Oxford, UK

Research Group Skirmantas Kriaucionis, Ludwig Institute for Cancer Research, Nuffield Department of Clinical Medicine, University of Oxford (UK)

- CRISP/Cas9 system II mediated mutagenesis of Tet proteins to establish a 5hmC deficient model system
- Experiments with TSA and observation of histone deacetylases in different ESC cultures
- Experiments with different ESC cultures under hypoxic conditions and observation of HIF1α

EDUCATION AND TRAINING

October 2013 – November 2015

Master of Science in Molecular Biology

ISCED 5A

University of Vienna – Universitätsring 1, 1010 Vienna (AUT)

- Compulsory elective subject: Cell Biology
- Neuroscience
- Microscopy
- Biochemistry
- Structure Biology
- Virology
- Stem Cells
- Epigenetic

September 2010 – June 2013

Bachelor of Science in Molecular Biotechnology

ISCED 5A

University of Applied Sciences – FH Campus Wien, Favoritenstraße 226, 1100 Vienna (AUT)

- Biology (Molecular Biology and Genetics, Genomics, Cell Biology, Cell Culture, Immunology, Developmental Biology, Microbiology, Histology, Human Physiology, Pharmacogenetics, Tissue Engineering, Biological Models)
- Chemistry (Analytical, Bioorganic, Inorganic, Organic, Physical, Biochemistry)
- Clinical Studies
- GMP & GLP
- Quality Management
- Project Management
- Bioinformatics
- Mathematics
- Statistics
- English in Science and Career
- Social Skill
- Law
- Product Management
- Marketing & Sales

PERSONAL SKILLS

Mother tongue: German

Other languages

	UNDERSTANDING		SPEAKING		WRITING
	Listening	Reading	Spoken interaction	Spoken production	
English	C2	C2	C1	C1	C1
	Cambridge Certificate in Advanced English (CAE)				
French	A2	B1	B1	A2	A2

Levels: A1/2: Basic user - B1/2: Independent user - C1/2 Proficient user
Common European Framework of Reference for Languages

Job-related skills

- Extensive practical skills acquired during my internship in Oxford, in Stockhom and my work at the Medical University Vienna
- Trained through supervisors (Oxford, Stockholm, Vienna) to critically evaluate obtained data and to set and design further experimental steps on my own
- Improved technical and practical skills during several laboratory exercises at the University of Applied Sciences (Cellular Biology, Molecular Biology, Biochemistry, Analytical Chemistry)

Communication skills

- Broad knowledge in conflict management, moderating, team building and presenting techniques due to the course Social Skills at the University of Applied Science

Organisational / managerial skills

- Leadership skills acquired through being responsible for a team of 15 people during a project at the University of Applied Science
- Achieved advanced self and team-organisational skills during the course "Project Management" at University of Applied Sciences
- Broadened self-organisational skills through training time and stress management in the course "Social Skills" at University of Applied Sciences

Computer skills

- Good knowledge of several relevant bioinformatical programmes (i.E. ApE, ImageQuant, Prism, ImageJ, Cell Profiler)
- Broad knowledge of the Microsoft Office Tools

Other skills

- Certificate for knowledge in economics
- Cambridge Certificate in Advanced English (CAE)